

# “Introduction to Grains, Phases, and Interfaces—an Interpretation of Microstructure,” *Trans. AIME*, 1948, vol. 175, pp. 15–51, by C.S. Smith

GREGORY S. ROHRER

DOI: 10.1007/s11661-010-0215-5

© The Minerals, Metals & Materials Society and ASM International 2010

SMITH’S seminal 1948 paper, “Grains, Phases, and Interfaces—an Interpretation of Microstructure,” has influenced scientists for six decades and continues to be a base upon which modern materials research is built. Because the current fashion is to measure a paper’s impact on the scientific community through its citations, I’ll begin by noting that as of January 2010, this paper has been cited 831 times since it was published (according to the ISI web of science). What is remarkable about these citations is that more than 100 of them occurred in the 4-year period between the start of 2006 and the end of 2009. This demonstrates that the paper has maintained its relevance to modern materials research 60 years after it was published. I do not doubt that in the future students of materials science will continue to read, and be inspired, by this work.

The basic idea put forth by Smith is that the geometry of a microstructure contains an “imprint” of the interfacial energies of the constituent solids and liquids. As a result, interfacial properties can be used to predict the microstructures that will be formed during materials processing and, conversely, relative interfacial properties can be determined from the interpretation of microstructures. The analysis is based upon the simple vector balance of interfacial energies at the junctions between misoriented crystals, different solid phases, solids and liquids, or solids and gasses. Within this framework, relative energies can be determined from the dihedral angles between interfaces, under the assumption of local

equilibrium usually obtained at high temperature during microstructure genesis. The entire analysis is illustrated by 30 beautiful optical micrographs.

One significant idea advanced by Smith in this paper is that grain boundary energies are anisotropic. While virtually nothing was known about grain boundary energies at the time, Smith argued for anisotropy on the basis dihedral angle measurements. Furthermore, from the observation that the junctions between twin boundaries and random grain boundaries, he realized that the former must have very low energies and that the latter must have an energy that depends on the boundary plane orientation. These conclusions, of course, have been proven to be accurate.

It is also noteworthy that while micrographs from plane sections are two-dimensional, real microstructures are three-dimensional. In the past, researchers frequently (and perhaps conveniently) overlooked this point. However, throughout the paper, Smith relates the two-dimensional information in his micrographs to plausible three-dimensional arrangements. In fact, after this paper, Smith pursued the first studies of three-dimensional grain shape using grain separation techniques and stereoscopic microradiography. This seems especially relevant today, as new tools such as the dual beam focused ion beam scanning electron microscope and high energy X-ray tomography make it possible for the first time to visualize the three-dimensional internal microstructures of materials.

---

GREGORY S. ROHRER, W.W. Mullins Professor and Head, is with the Department of Materials Science and Engineering, Carnegie Mellon University, 5000 Forbes Avenue Wean Hall 3325, Pittsburgh, PA. Contact e-mail: gr20@andrew.cmu.edu

Article published online March 17, 2010

# Grains, Phases, and Interfaces: An Interpretation of Microstructure

BY CYRIL STANLEY SMITH,\* MEMBER AIME

(Institute of Metals Division Lecture, New York Meeting, February 1948)

THE art of metallography is mature and the forms in which various micro-constituents appear are well known. Investigations almost without end have disclosed the importance of the exact manner of distribution of phases on the physical properties and usefulness of an alloy. Surprisingly, however, relatively little attention has been paid to the forces that are responsible for the particular and varied spatial arrangements of grains and phases that are observed. Like the anatomist, the metallurgist has been more concerned with form and function than with origins.

In this paper it is proposed to develop the simple concept that many microstructures result from an attempted approach to equilibrium between phase and grain interfaces whose surface tensions geometrically balance each other at the points and along the lines where they meet. From this follows a number of principles which may prove to be of interest to the metallographer and of practical use in explaining failures and in designing alloys for particular service. In general, the discussion will be limited to structures obtained after full annealing. The simple principles do not apply to structures resulting from Widmanstatten mechanisms in precipitation, or to other structures not in local equilibrium and in which lattice coherency is a determining factor.

## INTERFACIAL TENSION

Much has been written by physical chemists about the free energy of surfaces,

Manuscript received at the office of the Institute March 15, 1948. Issued as TP 2387 in METALS TECHNOLOGY, June 1948.

\* Director, Institute for the Study of Metals, University of Chicago.

which manifests itself as a measurable surface tension. Two- and three-phase interfaces in fluids seek a condition of minimum energy and approach a geometrical configuration in which the various forces are in vectorial balance.\* Measurement of the angles established between the interfaces when in equilibrium provides a quantitative value for the relative value of the surface forces involved. The case of two fluids meeting at the surface of a solid (of great importance in connection with the flotation of minerals) has often been studied, but there have been few investigations of the equally definite interface between two or more crystals of a single solid phase, or the more complex cases where crystal grains of more than one phase are involved.

The principles are best illustrated by considering first the case of two and three immiscible liquids. If, as in Fig 1, a liquid, 2, is dropped into a less dense liquid, 1, it will form a sphere—if gravity and viscosity can be ignored—for in this shape the interface has the smallest possible area. If these two phases should together encounter a third phase in which they are both immiscible, the geometry will change to become that which gives the lowest total energy for all three interfaces. Thus, if the spherical drop of liquid, falling through 1, eventually reaches the interface between liquids 3 and 1 (we are assuming that the density of 3 is greater than 2, and 2 than 1), it will assume the shape of a lens, the angle

\* N. K. Adams: *Physics and Chemistry of Surfaces* (Oxford, Clarendon Press, 1941). provides a readable and complete description of surface phenomena and their interpretation.

at the edge being that needed to establish equilibrium between the tensions in the three different interfaces. The angle is exactly the same as that established by three strings passing from a knot indi-

ume and to the limitations imposed by other junctions and by the external boundaries of the system. Gravity will distort the shapes unless the volumes or the density differences concerned are very small.

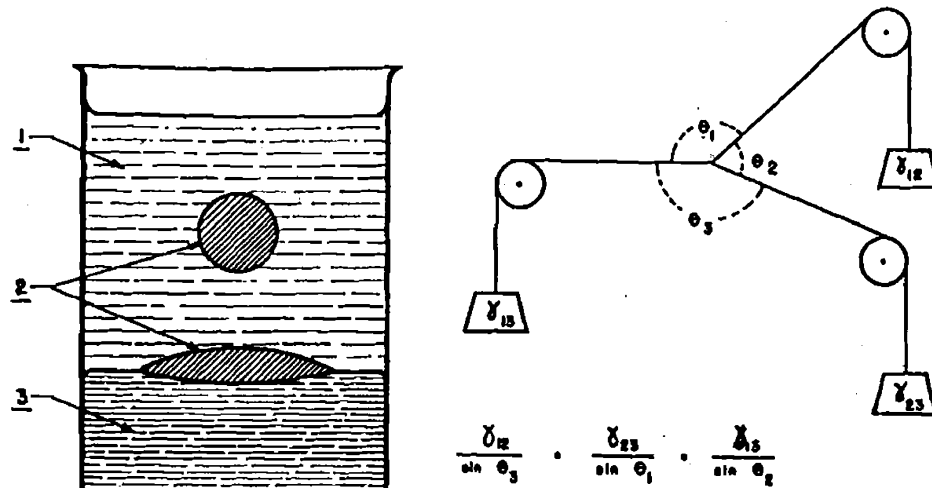


FIG 1.—INTERFACE EQUILIBRIUM BETWEEN THREE IMMISCIBLE LIQUIDS AND MECHANICAL ANALOGY WITH TRIANGLE OF FORCES.

vidually over pulleys and carrying weights in the same ratio as the interface tensions. This is shown diagrammatically on the right of Fig 1. It follows from elementary mechanics that any one of three forces in equilibrium is equal in value and opposite in direction to the resultant of the other two. In Fig 1,  $\gamma_{12}$ ,  $\gamma_{13}$ , and  $\gamma_{23}$  represent the various interface tensions at the three-phase junction, and  $\theta_1$ ,  $\theta_2$ , and  $\theta_3$  the angles occupied by phases 1, 2, and 3 where they meet. By the use of the triangle of forces we then have the relations

$$\frac{\gamma_{23}}{\sin \theta_1} = \frac{\gamma_{13}}{\sin \theta_2} = \frac{\gamma_{12}}{\sin \theta_3}$$

The three interfacial tensions are therefore in the same ratio as the sines of the angles subtended by the phase opposite each particular interface. These angles will be attained at every point along the line of junction and must be measured in a plane normal to it. In most real systems the surfaces away from this line will be curved in a manner to attain minimum total surface energy with due regard to the fixed vol-

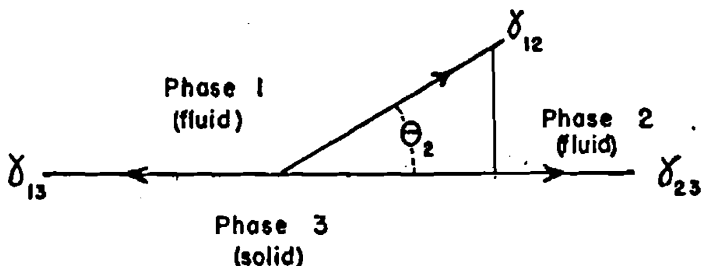
If one of the phases is rigid and plane, and the other two are fluid, as in Fig 2, the resultant of the tension of the fluid-fluid interface acting in the plane surface must be equal to the difference between the interfacial tensions of the two liquids against the solid, that is,  $\gamma_{13} - \gamma_{23} = \gamma_{12} \cos \theta_2$ .

This equation cannot be satisfied if  $\gamma_{12}$  is less than  $\gamma_{13} - \gamma_{23}$ . When this occurs, phase 2 spreads indefinitely over the surface of the solid and entirely displaces phase 1. This is the case of complete wetting. In a capillary or in a porous medium or powder, liquid 2 will displace 1 when  $\theta_2$  is less than  $90^\circ$  because of the curvature introduced by opposing faces. Metallurgists are familiar with this effect in the spreading of solder. For example, Parker and Smoluchowski<sup>1</sup> have shown that silver will not spread indefinitely on a plane iron surface (where it has apparently a small but positive contact angle) but will spread on a grooved surface—more readily the more acute the angle at the root of the grooves.

<sup>1</sup> References are at the end of the paper.

Copper, with zero contact angle, spreads indefinitely over a steel surface. It is the contact angle that allows molten metal to rest on a sand mold, but causes water to be

irrelevant to the conclusions though it would determine the rate of attainment of equilibrium. Three possible means have been suggested: diffusion of atoms in the



$$\gamma_{13} - \gamma_{23} = \gamma_{12} \cdot \cos \theta_2$$

FIG 2—INTERFACE EQUILIBRIUM BETWEEN TWO LIQUIDS AT A SOLID SURFACE.

drawn in rapidly; oil will soak into sandstone but water will entirely replace it. Many molten metals will be soaked up into a loose compact of another metal powder of higher melting point, because of low contact angle, but this is not invariably the case. The success of the porous nickel cups used in the safety switch in the new proximity fuses<sup>2</sup> is probably due to the fact that the contact angle of mercury against nickel is slightly more than 90°, so that, although it will not penetrate the relatively large pores of the nickel compact under ordinary conditions, the extra pressure provided by centrifugal force on firing the shell causes it to do so.

Let us now consider the situation where three solid phases meet in a manner similar to the fluids of Fig 1. If the solids are truly rigid, clearly there will be no change in shape, but if adjustment can occur, however slowly, the three phases will eventually reach the configuration dictated by the balance of the interfacial tensions. It is a basic assumption in what follows that in solid metals at a sufficiently high temperature, displacement of matter can and does occur, and that this proceeds until local equilibrium is established wherever grains and phases meet. The mechanism whereby this adjustment of angle is achieved is

normal way through the crystals under the influence of the different escaping tendencies of atoms on differently curved faces; rapid diffusion along the interfaces; and creep, that is, actual plastic deformation occurring under the influence of unbalanced surface forces.

In liquids, phase boundaries provide the only possible interfaces. In the case of solids, however, there is the important distinction that it is possible to have a definite interface between two regions of the same phase—the grain boundary between two crystals differing only in orientation. This boundary behaves in the same manner as a normal interface between different phases; it is extendable, continuous, and has a definite free energy associated with each unit of area. It might be expected that the energy would be strongly dependent on the orientation difference across the boundary. However, the shape of the grain boundaries in most metals suggests that there is actually only a relatively small effect of orientation, except for the low energy associated with the highly critical matching of orientations corresponding to a twin.

If the tensions of all grain boundaries are approximately equal, wherever three grains meet they will establish equilibrium with

their boundaries making equal angles of  $120^\circ$  with one another. When four grains meet at a point, the four edges will make the tetrahedral angle of  $109^\circ 20'$  with one

ilibrium with the two interphase boundaries, and the angles, measured in the plane normal to the line of intersection, will be determined by the relative values of the

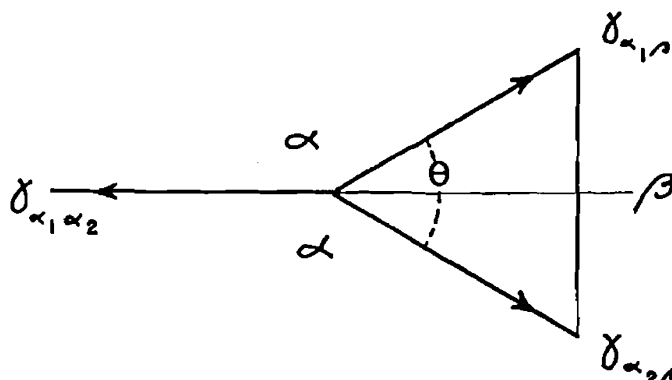


FIG 3—EQUILIBRIUM BETWEEN A GRAIN BOUNDARY AND TWO EQUAL INTERPHASE BOUNDARIES.  
 $\theta$  IS THE DIHEDRAL ANGLE.

another. As Harker and Parker<sup>3</sup> have shown, the accidents of distribution in any real metal will result in the introduction of curvatures to reconcile the various random grain contacts with these angles—of which more later when we come to consider grain growth.

Let us examine the more interesting case where interfaces between grains of different phases are concerned. In the absence of any crystal boundaries in either phase, the boundary of one phase when completely surrounded by another must eventually become a sphere, for this is the smallest surface to contain a fixed volume. Any departure from an exactly spherical equilibrium shape must be caused by a variation of interface energy with orientation, and provides, indeed, a good way of determining this seemingly small effect. If there are three interfaces present, regardless of whether these are interphase or intercrystal boundaries, then equilibrium will be established at whatever configuration results in the minimum surface energy for the given conditions. If there are two crystals of one phase meeting with one crystal of a second phase, the one grain boundary will establish geometric equi-

interfacial tensions. In Fig 3, assuming that the two interphase boundaries are not subject to crystallographic influences, so that  $\gamma_{\alpha:\beta} = \gamma_{\alpha,\beta} = \gamma_{\alpha\beta}$  then

$$\gamma_{\alpha_1\alpha_2} = 2\gamma_{\alpha\beta} \cos \frac{\theta}{2t}$$

Fig 4 shows the value of the ratio of the two interfaces for angles  $\theta$  between  $0$  and  $180^\circ$ . It is obvious from this that if the interphase boundary tension is more than half that of the grain boundary in one phase,  $\theta$  will be positive; if the tensions are equal,  $\theta$  will be  $120^\circ$ ; and if the interphase boundary tension exceeds the grain boundary tension,  $\theta$  will be more than  $120^\circ$ . If the interphase tension energy is less than half that of the grain boundary, there is no value of  $\theta$  that can satisfy the equation and the second phase will penetrate along the boundary indefinitely. Fig 5 shows in an idealized form the shapes, for various values of  $\theta$ , that a small volume of a second phase must have if it appears at the corner of three grains.

This angle  $\theta$  will hereafter be called the *dihedral angle*, specifically in Fig 3 the

" $\beta$  vs  $\alpha/\alpha$  dihedral angle." The notation for other grain boundaries and phase interfaces will be obvious. The dihedral angle is constant and reproducible for a given pair

where  $\theta$  is the true dihedral angle,  $\phi$  the observed angle on a plane of section whose normal makes an angle  $\chi$  with the line of intersection of the two planes, and where  $\psi$

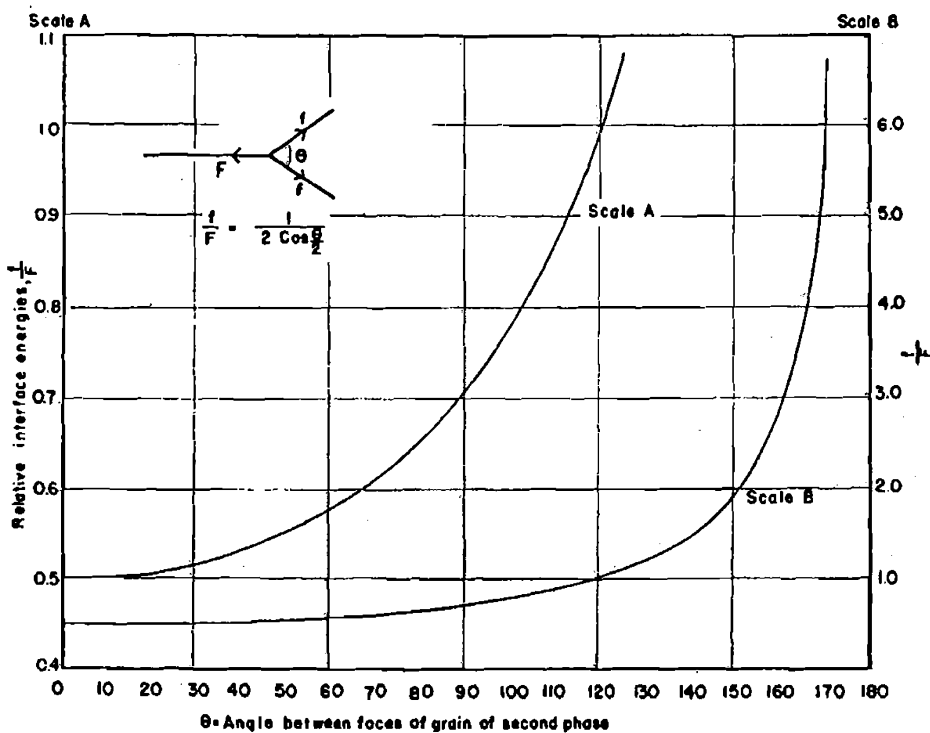


FIG 4—RATIO OF INTERPHASE BOUNDARY TENSION AND GRAIN BOUNDARY TENSION AS A FUNCTION OF DIHEDRAL ANGLE OF SECOND PHASE.

of phases, for it is determined only by the relative values of interphase and intergrain boundary tensions. Depending on its value, an alloy with more than one phase will assume one or other of the types of microstructure familiar to the metallgrapher.

Remember that the usual metallographic microsample is a plane section cut at random through a three-dimensional structure, and that an angle between two planes may appear on this section as any value between  $0^\circ$  and  $180^\circ$ , though with greatly differing probabilities. The angle at any intersecting plane can be calculated by the formula given by Harker and Parker,<sup>1</sup> namely,

$$\tan \phi = \frac{2 \sin \theta \cos \chi}{\sin^2 \chi (\cos 2\chi - \cos \theta) + 2 \cos \theta}$$

is the angle that the projection of this normal makes with the bisectrix of  $\theta$  in the plane perpendicular to the line of intersection—that is,  $\chi$  and  $\psi$  are the latitude and longitude, respectively, of the point of intersection of the normal in a reference sphere. Curves derived from this formula,\* using the graphical integration method proposed by Harker and Parker, are shown in Fig 6. They show for various dihedral angles the probability of obtaining on a random plane section an angle within  $\pm 5^\circ$  of the value plotted. These will be used for comparison with actual measurements given later. Note that, despite asymmetry except in the case  $\theta = 90^\circ$ , the most probable angle is in every instance the true dihedral angle. There is no error in assum-

\* The author wishes to thank Mr. Daniel Orloff for making these calculations.

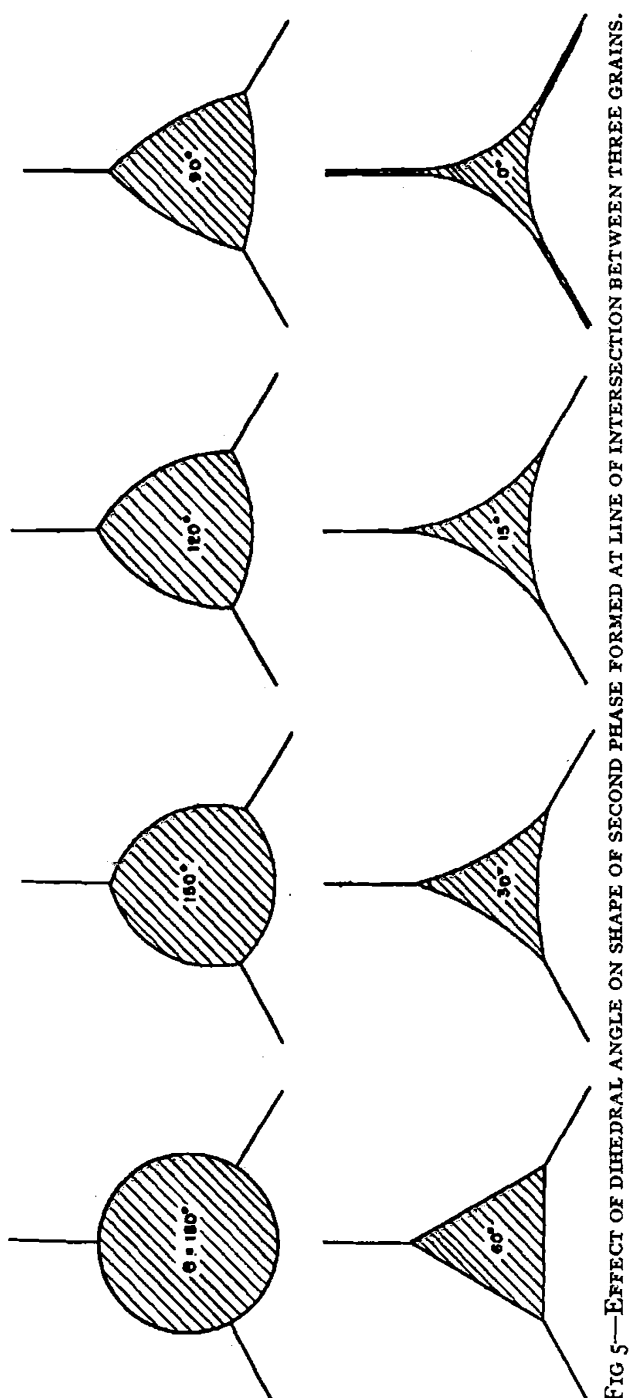


FIG 5—EFFECT OF DIHEDRAL ANGLE ON SHAPE OF SECOND PHASE FORMED AT LINE OF INTERSECTION BETWEEN THREE GRAINS.

ing  $\theta$  to be the angle most frequently observed.

We are now ready to consider the application of these principles to microstructures actually observed in metals and alloys.

#### MICROSTRUCTURES OF TWO-PHASE ALLOYS

Fig 7 to 12 show some microstructures of several common types. Fig 7 shows the

typical polygonal grain structure of a single metal phase—in this case annealed alpha iron. Fig 8 shows twinned grains of alpha brass after working and annealing. (The straight lines are twin boundaries and should be ignored for the present.)

In Fig 9 (a Cu-Ag solid solution annealed just above the solidus and quenched) the dihedral angle is obviously zero, for the

second phase (liquid) has spread along all grain boundaries and almost completely isolates the grains. In Fig 10 to 14 (alpha-beta brass, alpha-beta bronze, and alpha-

Fig 16 is an interesting case. It shows the structure of an alloy of copper with 3 pct lead, cold rolled and annealed at 900°C. The small amount of lead, molten at the

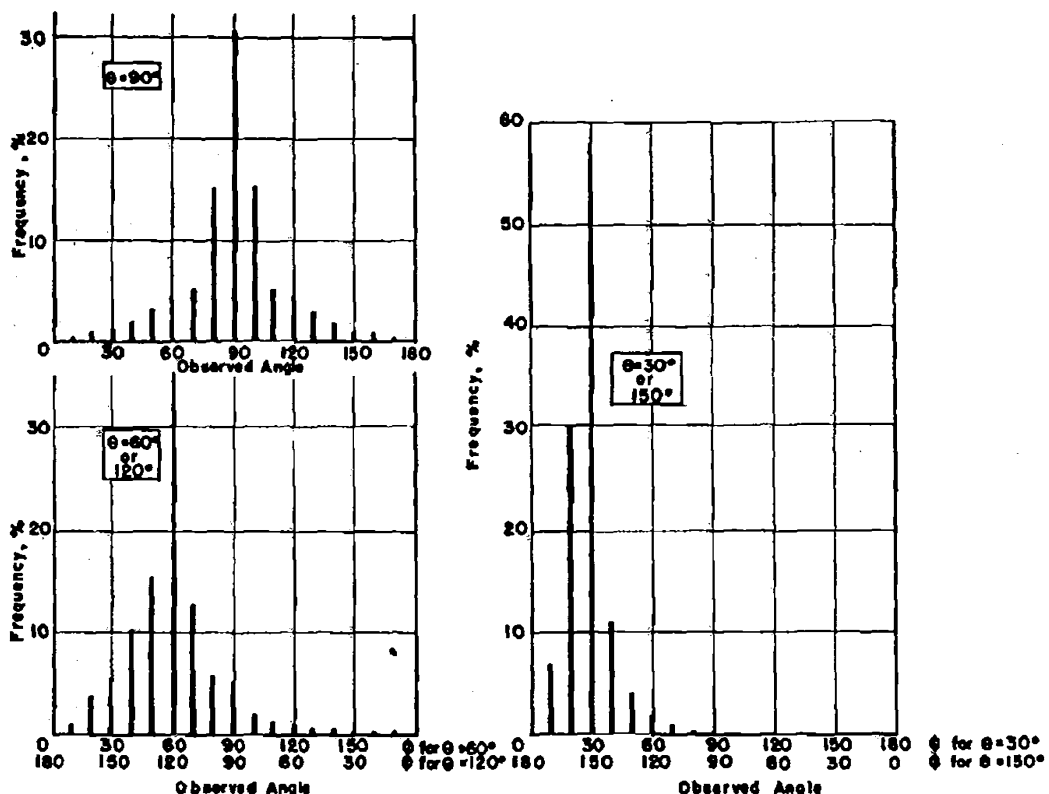


FIG 6—THEORETICAL FREQUENCY OF OBSERVED ANGLES,  $\phi$ , ON RANDOMLY INTERSECTING PLANE AS A FUNCTION OF TRUE DIHEDRAL ANGLE,  $\theta$ .

gamma iron) the tension of the boundary between the grains of different phases is less than that of the alpha grain boundary but more than half. The grains of the second phase are sharply pointed wherever they meet an alpha grain boundary, which they do at a clearly defined dihedral angle, 100° in the case of brass and 90° with steel. In Fig 15 (alpha iron plus cementite), the second phase is more nearly spherical in shape, with slight projections where it meets a grain boundary. The dihedral angle is 115°. The difference between the structures shown in the various micrographs, Fig 7 to 15, is principally due to differences in the dihedral angles. Table I records the measured dihedral angles of these and a number of other two- and three-phase alloys.

time of anneal, has collected into little triangles at the grain corners, the dihedral angle being about 60° and very readily and reproducibly measured. Fig 17 shows clearly that a lead drop that is not associated with a grain boundary remains very nearly spherical—an indication, incidentally, that the surface energy of the crystal-liquid interface is not appreciably dependent on the orientation of the solid face.

The reader must again be reminded that the structures are three-dimensional and that the metallurgist's microsection is a random two-dimensional slice. What appear in Fig 16 as small triangles at a three-grain corner are actually triangular prisms extending along the edges where three grains would otherwise meet (Fig 18).

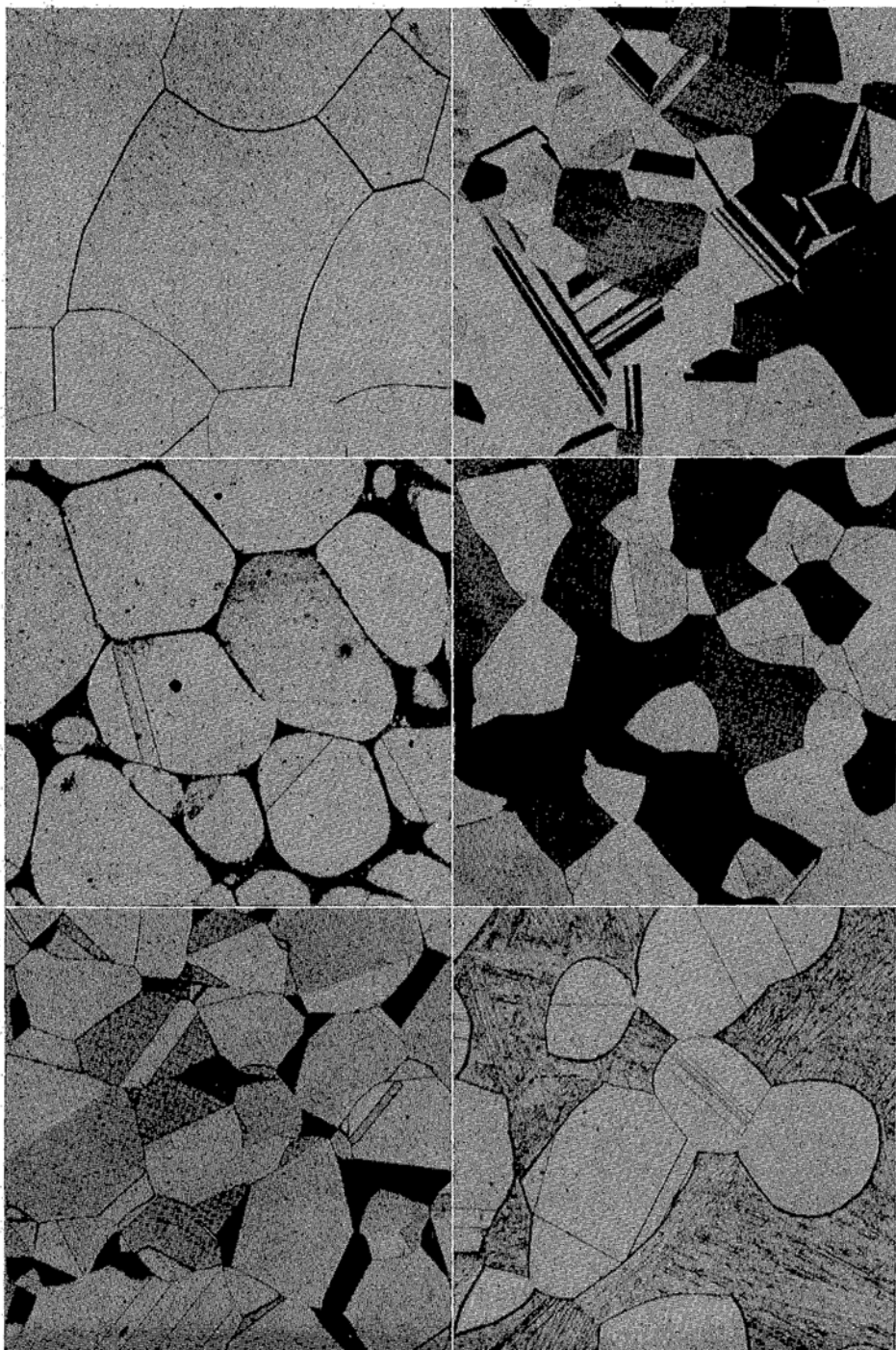


FIG 7—(607-1) POLYGONAL GRAINS IN ANNEALED IRON. ("PURON." ANNEALED 1,000 MIN., 850°C. NITAL ETCH.  $\times 250$ .)

FIG 8—(801-1) TWINNED POLYGONAL GRAINS IN ANNEALED ALPHA BRASS (70-30 Cu-Zn, 0.1 MM THICK, 0.12 MM GRAIN SIZE. AMMONIA AND PEROXIDE ETCH.  $\times 100$ ).

FIG 9—(788-B3) PARTLY MELTED SILVER-COPPER ALLOY (15 PCT AG, QUENCHED FROM 850°C. DICHROMATE ETCH.  $\times 250$ ).

FIG 10—(874-1) ALPHA-BETA BRASS (60-40 Cu-Zn ANNEALED 4 DAYS AT 700°C, QUENCHED. DICHROMATE AND FERRIC CHLORIDE ETCHES.  $\times 100$ ).

FIG 11—(872-1) ALPHA-BETA BRASS (63-37 Cu-Zn, ANNEALED 4 DAYS AT 700°C, QUENCHED. DICHROMATE AND FERRIC CHLORIDE ETCHES.  $\times 100$ ).

FIG 12—(700-1) ALPHA-BETA BRONZE (79-21 Cu-Sn, ANNEALED 2 HR AT 750°C, QUENCHED. DICHROMATE ETCH.  $\times 250$ ).

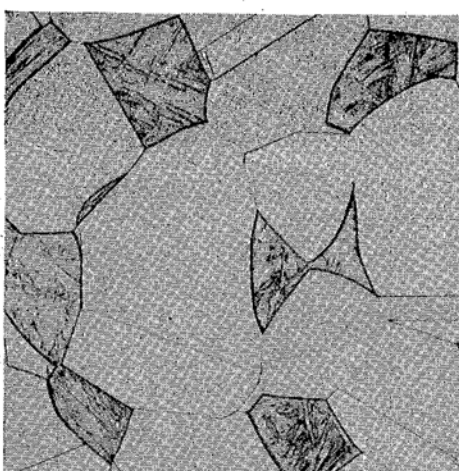


FIG 13

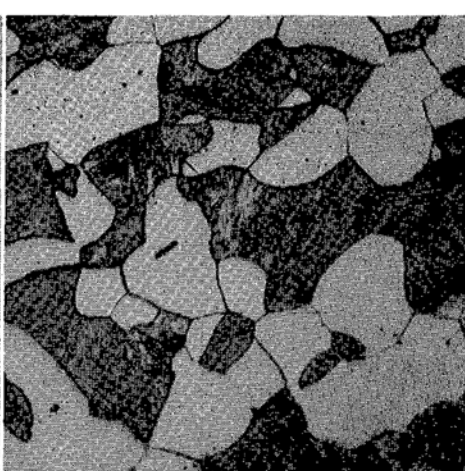


FIG 14

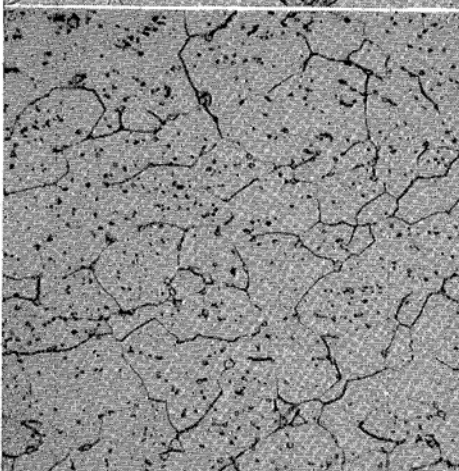


FIG 15

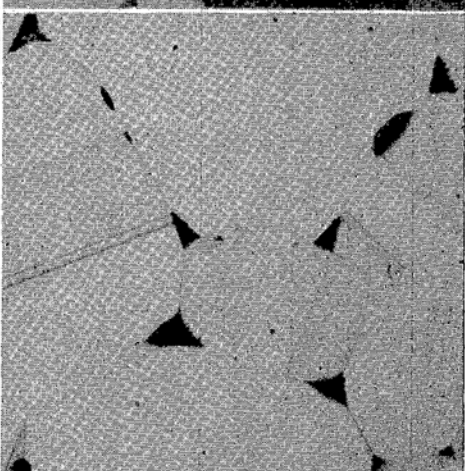


FIG 16

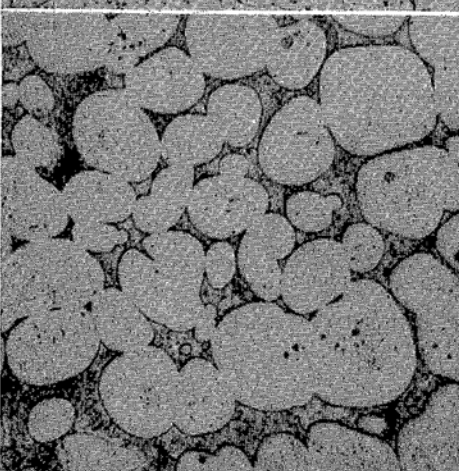


FIG 21

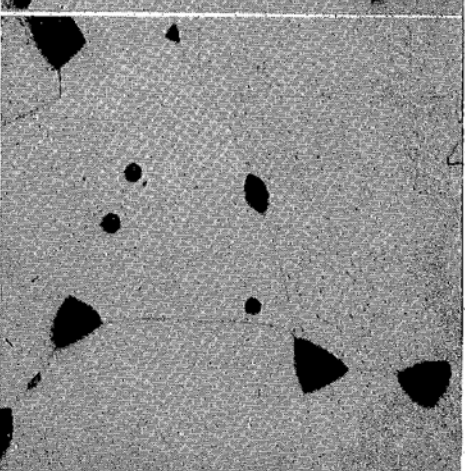


FIG 22

FIG 13—(699-1) ALPHA-BETA BRONZE (84-16 Cu-Sn, ANNEALED 2 HR AT 750°C, QUENCHED, DICHROMATE ETCH.  $\times 250$ ).

FIG 14—(844-1) FERRITE + TRANSFORMED AUSTENITE (S.A.E. 1020 STEEL, ANNEALED 24 HR AT 750°C, QUENCHED, NITAL ETCH.  $\times 500$ ).

FIG 15—(863-1) FERRITE + CEMENTITE. (S.A.E. 1020 STEEL ANNEALED 1 WEEK AT 680°C, QUENCHED. NITAL ETCH.  $\times 500$ ).

FIG 16—(736-3A) COPPER + LIQUID LEAD (97-3 Cu-Pb, ANNEALED 1 HR AT 900°C. DICHROMATE ETCH.  $\times 500$ ).

FIG 21—(848-1) IRON + LIQUID PHASE IN IRON-COPPER ALLOY (70-30 Fe-Cu; FORGED, ANNEALED 1 HR AT 1125°C, QUENCHED. AMMONIA AND PEROXIDE ETCH.  $\times 500$ ).

FIG 22—(793-1) ALPHA + LIQUID IN LEADED BRASS (67-30-3 Cu-Zn-Pb. ANNEALED 16 HR AT 750°C, QUENCHED. DICHROMATE ETCH.  $\times 500$ ).

The prisms join smoothly into each other at four-grain junctions, always keeping the correct dihedral angle. The conditions of stability of such prisms are not simple. A

adjacent grain boundary tension, the resulting triangular shape becomes stable at longer and longer lengths until, at a dihedral angle of  $60^\circ$  and below, the phase

TABLE I—*Experimental Values of Dihedral Angle in Two- and Three-phase Alloys*

No.	Composition	Treatment	Dihedral Angle	Ratio of Interfacial Tensions
A-920-C	60 Cu, 40 Zn	24 hr 600°C	$\alpha$ vs. $\beta/\beta$ 120°	1.00
	60 Cu, 40 Zn	24 hr 600°C	$\beta$ vs. $\alpha/\alpha$ 100°	0.78
A-920-K	60 Cu, 40 Zn	4 days 700°C	$\alpha$ vs. $\beta/\beta$ 120°	1.00
	60 Cu, 40 Zn	4 days 700°C	$\beta$ vs. $\alpha/\alpha$ 100°	0.78
A-918-B	63 Cu, 37 Zn	8 hr 700°C	$\beta$ vs. $\alpha/\alpha$ 70°	0.61
A-2117	91 Cu, 9 Al	850° Furn.C., 48 hr 600°C	$\beta$ vs. $\alpha/\alpha$ 90°	0.71
A-2119	86 Cu, 14 Al	850° Furn.C., 48 hr 600°C	$\beta$ vs. $\gamma/\gamma$ 110°	0.87
A-391	79 Cu, 21 Sn	2 hr 700°C	$\alpha$ vs. $\beta/\beta$ 110°	0.87
A-2105-A	79 Cu, 21 Sn	2 hr 750°C	$\beta$ vs. $\alpha/\alpha$ 100°	0.78
A-2105	84 Cu, 12 Sn	2 hr 750°C	$\beta$ vs. $\alpha/\alpha$ 95°	0.74
A-2133-B	79 Cu, 17 Sn, 4 Pb	750° Furn.C., 24 hr 600°C	$\alpha$ vs. $\beta/\beta$ 120°	1.00
	79 Cu, 17 Sn, 4 Pb	750° Furn.C., 24 hr 600°C	$\beta$ vs. $\alpha/\alpha$ 95°	0.74
	79 Cu, 17 Sn, 4 Pb	750° Furn.C., 24 hr 600°C	Pb vs. $\alpha/\alpha$ 90°	0.71
	79 Cu, 17 Sn, 4 Pb	750° Furn.C., 24 hr 600°C	Pb vs. $\beta/\beta$ 110°	0.87
	79 Cu, 17 Sn, 4 Pb	750° Furn.C., 24 hr 600°C	$\alpha/\beta$ vs. Pb $\beta$ vs. Pb $\alpha$ 110, 120, 130	
A-2106-A	99 Cu, 1 Pb	2 hr 700°C	Pb vs. $\alpha/\alpha$ 65°	0.59
A-2106-B	99 Cu, 1 Pb	1 hr 900°C	Pb vs. $\alpha/\alpha$ 50°	0.55
A-2106-G	99 Cu, 1 Pb	14 hr 600°C	Pb vs. $\alpha/\alpha$ 60°	0.58
A-2172-C	97 Cu, 3 Pb	24 hr 600°C	Pb vs. $\alpha/\alpha$ 70°	0.61
A-2145-A	99 Cu, $\frac{1}{2}$ Bi, $\frac{1}{2}$ Pb	16 hr 750°C	Liq. vs. $\alpha/\alpha$ 55°	0.56
A-2151-C	99 Cu, $\frac{1}{2}$ Bi, $\frac{1}{2}$ Pb	16 hr 750°C	Liq. vs. $\alpha/\alpha$ 40°	0.53
A-2144-A	99 Cu, $\frac{3}{4}$ Bi, $\frac{1}{4}$ Pb	16 hr 750°C	Liq. vs. $\alpha/\alpha$ 30°	0.52
A-2175-B	95 Cu, 2 Zn, 3 Pb	24 hr 650°C	Liq. vs. $\alpha/\alpha$ 70°	0.61
A-2176-B	88 Cu, 9 Zn, 3 Pb	24 hr 650°C	Liq. vs. $\alpha/\alpha$ 80°	0.65
A-2177-B	78 Cu, 19 Zn, 3 Pb	24 hr 650°C	Liq. vs. $\alpha/\alpha$ 80°	0.65
A-2153-B	68 Cu, 29 Zn, 3 Pb	16 hr 750°C	Liq. vs. $\alpha/\alpha$ 80°	0.65
A-2155	49 Cu, 48 Zn, 3 Pb	16 hr 700°C	Liq. vs. $\beta/\beta$ 110°	0.87
A-2113-C	SAE 1020 Steel	950° Furn.C., 1 wk. 690°	Fe <sup>3</sup> C vs. $\alpha/\alpha$ 115°	0.93
A-2113-D	SAE 1020 Steel	950° Furn.C., 48 hr 750°	$\gamma$ vs. $\alpha/\alpha$ 90°	0.71
A-2069-B	70 Fe, 30 Cu	1 hr 1125°C	Liq. vs. $\gamma/\gamma$ 20°	0.31
A-2104-A	90 Zn, 6 Cu, 4 Al	48 hr 375°C	$\eta$ vs. $\epsilon/\epsilon$ 115° $\eta$ vs. $\beta/\beta$ 120° $\epsilon$ vs. $\eta/\eta$ 115° $\epsilon$ vs. $\beta/\beta$ 110° $\beta$ vs. $\eta/\eta$ 110° $\beta$ vs. $\epsilon/\epsilon$ 95°	0.93 1.00 0.93 0.87 0.87 0.74

In order to cause recrystallization, all alloys were rolled or forged at least 50 pct reduction before final heat treatment. Specimens were quenched at termination of anneal. Many of these alloys were heat treated for long periods to reach substantial equilibrium of grain and interphase boundaries. The angles are approximately the same after short anneals but are more difficult to measure because of curvature. The angles were measured by rotation of the stage of a B and L metallograph to align the appropriate boundaries successively with a fixed cross-hair. At least 100, usually 200, counts were made.

cylinder supported on rings at its ends is not stable when acted upon by surface tension if its length exceeds its circumference, but it will break up into drops. If the second phase forming at a grain edge in an alloy has a dihedral angle against the grain boundaries of nearly  $180^\circ$ , it will behave like a cylinder and will certainly break up. Such a phase will appear as a chain of nearly spherical drops along the boundary—not unlike a string of dewdrops on a spider web. If, however, the interphase tension is low in comparison with the

becomes stable in any length at a grain edge.

The precise shape in three dimensions of the interface between a particle of a second phase and the various grain surfaces and edges is a matter of great complexity. The sphere of a second phase which exists within the body of a grain, when it touches a plane boundary between two grains, becomes a simple lenticulate body; in the absence of gravity the two surfaces become sections of spheres intersecting at the correct dihedral angle at the edge. If a particle

occurs at a line where three grains meet, the three interphase edges (e.g., edges where one  $\beta$  grain meets two  $\alpha$  grains) will make equal angles with each other and each will be equally inclined to the single phase grain

three  $\alpha$  grains meet) is given by the relation

$$\cos(180 - Y) = \frac{1}{\sqrt{3} \tan \frac{\theta}{2}}$$

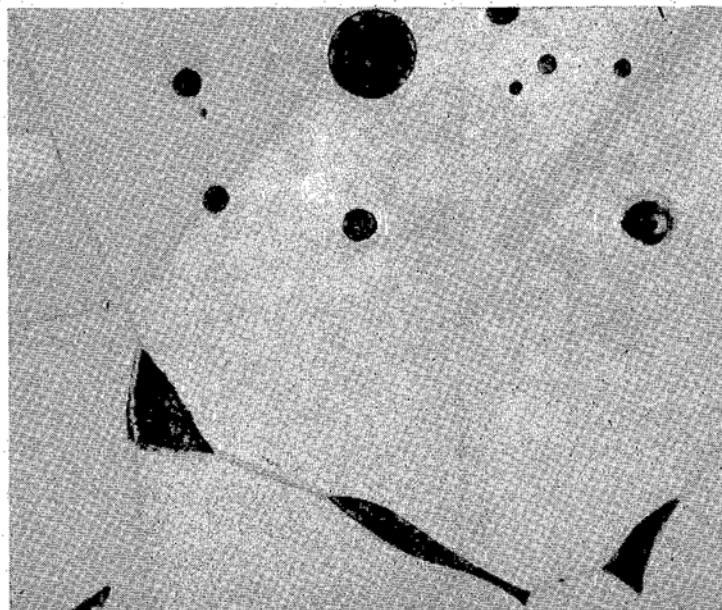


FIG 17—(736-3D) COPPER + LIQUID LEAD. NOTE CIRCULAR CROSS-SECTION OF LIQUID DROPS IN CENTER OF GRAIN AND TRIANGULAR SHAPE AT GRAIN CORNER. (SAME SPECIMEN AS FIG 16; DIFFERENT FIELD.  $\times 1000$ .)

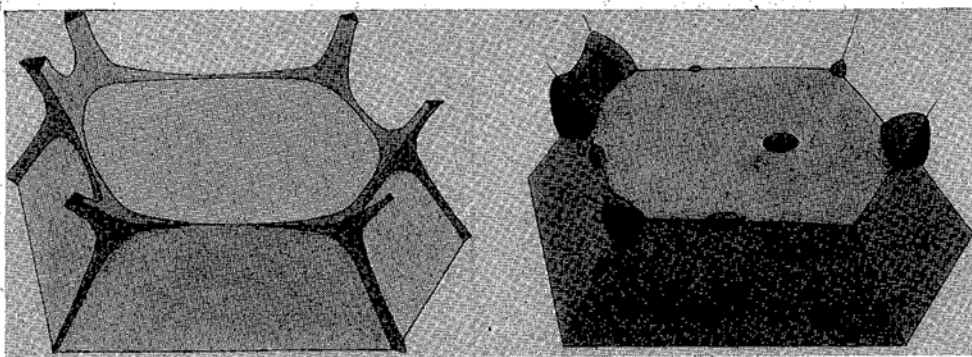


FIG 18—SKETCH SHOWING DISTRIBUTION OF SECOND PHASE IN THREE DIMENSIONS. LEFT  $\theta$  = ABOUT  $65^\circ$ , RIGHT  $\theta$  = ABOUT  $120^\circ$ .  
(Drawing by C. S. Barrett.)

edge. The angle,  $X$ , in Fig 19 between polyphase edges of one face at the apex of the second phase for a given dihedral angle,  $\theta$ , is given by the relation

$$\cos \frac{X}{2} = \frac{1}{2 \sin \theta_2}$$

The angle,  $Y$ , between each polyphase edge and the single phase grain edge (i.e., where

Curves showing these relations are plotted in Fig 20. When  $\theta = 120^\circ$ ,  $X = Y = 109^\circ 20'$ . This is the geometry of the corner of four grains of the same phase. When  $\theta = 60^\circ$ ,  $X = 0^\circ$  and  $Y = 180^\circ$ ; the pyramid has become a triangular prism extending without limit. At any dihedral angle of less than  $60^\circ$  the phase will spread indefinitely along the grain edge (not, of

course, along the grain faces which requires  $\theta = 0^\circ$ ), while with a dihedral angle of over  $60^\circ$  the second phase will collect at grain corners and extend progressively less along

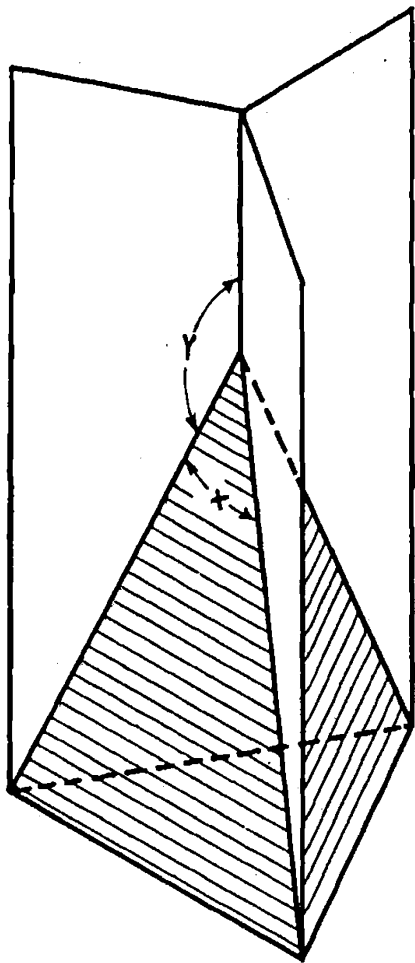


FIG 19—IDEALIZED APPEARANCE OF APEX OF SECOND PHASE FORMING AT THE JUNCTION OF THREE GRAINS.

the boundary as  $\theta$  increases, becoming more and more spherical. Complex curvature will be introduced to join up the various contacts and angles in a manner to give minimum total interface energy for the volumes concerned. Nevertheless, the dihedral angle measured normal to the line of junction at any point will invariably be the true, simple dihedral angle called for by the relative interface tensions.

A second phase will always show greatest preference for the points where four grain corners join, since it can then partially

replace six surfaces, and there is progressively less decrease in total interface area as the second phase is associated with a three-grain edge and a two-grain surface. The gain in energy when phase and grain boundaries coincide becomes proportionately less as the dihedral angle increases, and phases of high interfacial tension show less preference for boundaries. Phases of low dihedral angles appear much more frequently in association with grain boundaries and corners than do phases of high angles and interface energies. A phase of low interface energy cannot spheroidize when it is at a grain boundary of higher energy. The higher the dihedral angle, the more nearly spherical a particle of the second phase will be, and the less its change in shape and energy when it encounters a grain boundary. Conversely, whatever the initial distribution of a phase of low dihedral angle, it will spread out whenever it meets a grain boundary, and will be picked up by the latter as it migrates during grain growth. Once collected at a grain boundary, such a phase will move only with the boundary, and the boundary will move only with it. In a recrystallized solid solution annealed briefly just above the solidus, one sees liquid both as films at the grain boundaries and as drops inside the grains; annealing to double the grain size will show in some of the larger grains areas that have been swept free from liquid droplets by advancing boundaries. Very long annealing, to cause the grains to grow to several times the original size and to allow transfer by diffusion, will result in grains quite free from liquid drops, and with all the liquid phase collected at grain corners and boundaries.

The behavior of a phase with high dihedral angle is quite different. Not only does its mere geometry as small independent near-spheres prevent coordinated action of a large amount of material, but the change of surface energy resulting from

the coincidence of grain and phase boundary is small. The grain boundary can pass fairly easily one at a time over a series of small spheres, the energy of the localized

large difference in atom size or otherwise, two metals are immiscible when molten, the interfacial tension between the two liquids is high, and when one of them has solidified,

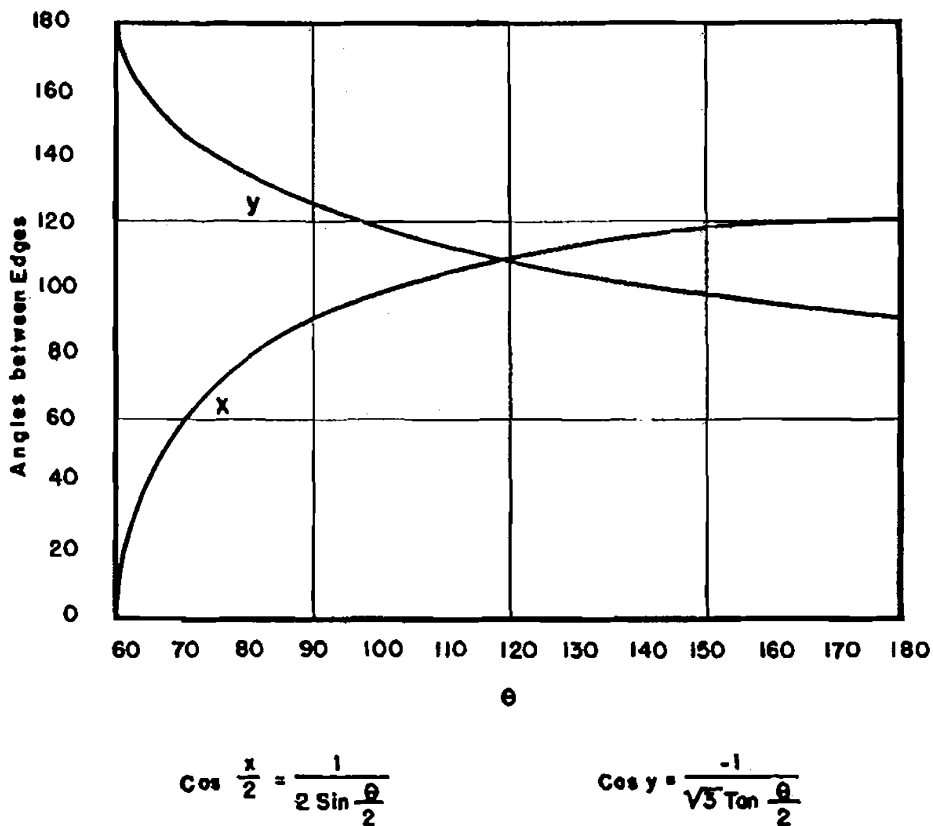


FIG 20—ANGLES BETWEEN GRAIN EDGES AT POINT WHERE A GRAIN OF ONE PHASE MEETS THREE GRAINS OF A SECOND.

(X = angle between adjacent 2-phase edges; Y = angle between 1-phase and 2-phase edges. See Fig 19.)

areas held back by surface energy forces being small compared with the whole area of the grain face concerned.

#### DISTRIBUTION OF LIQUID PHASES IN ALLOYS

In pure metals and in alloy systems where extensive solid solutions or intermetallic compounds occur and the liquid does not differ widely in composition from the solid, it seems to be invariably true that the liquid will "wet" the grains of the solid phase with which it is in equilibrium. This means that the interfacial tension of the solid/liquid interface is less than half that of the interface between two solid grains, and the dihedral angle of the liquid vs. grain boundary is zero. If, because of

the solid/liquid interface tension may easily exceed half of that of the boundary between two solid grains. Thus, for example, while a partly melted copper-silver alloy (Fig 9) shows the grains with rounded corners completely surrounded by films of liquid, a partly melted lead-zinc alloy shows a normal grain structure and drops of lead almost at random throughout. The copper-lead alloy of Fig 16 is intermediate.

It has long been known to practical metallurgists that overheating an alloy produces liquid with a great preference for the grain boundaries and with often disastrous effects on the properties. The hot-shortness of steels and many non-

ferrous alloys with common impurities is directly attributable to the presence of liquid that wets grain boundaries. The easy penetration of mercury into brass under low stresses and the similar cracking of steel by molten brazing solder are related to this. The temperature at which extreme brittleness suddenly appears is a sensitive method of determining the solidus of an alloy. Nevertheless, many cases are known where liquids are *not* harmful, for example, lead in beta brass and fusible silicates (but not always sulphides) in steel. Lead added in reasonable amounts to copper or alpha brass will cause cracking on hot rolling but it does not make the metal sufficiently hot-short to interfere with extrusion, neither does it have much effect on the ductility and strength at room temperature. As can be seen from Fig 16 and 17, lead has a small but definite dihedral angle against grain boundaries in copper and forms, not harmful continuous layers of liquid, but little prisms at the grain edges. Certainly its effect as a stress-raiser is bad and the lack of hot rollability is not surprising, but the lead does not interfere with crystal-to-crystal cohesion.

Table 1 contains data showing the change of behavior of lead with zinc content in copper-zinc alloys. The observed distribution of angles can be seen in Fig 27. As zinc increases, the dihedral angle of liquid lead vs. an alpha grain boundary increases, the corners of the lead areas become more blunt, and there is less tendency to form long prisms at the edges. With above 10 pct zinc ( $\theta = 80^\circ$ ) the grain corner prisms have become convex, there are many disconnected drops on boundaries away from corners, and a few drops appear entirely divorced from the boundaries, particularly after short annealing times (Fig 22). As a consequence, lead does not have a harmful effect on the mechanical properties of alpha brass at room temperatures. When beta appears, the distribution of lead abruptly changes. The dihedral

angle of molten lead vs. a beta grain boundary is about  $110^\circ$ , consequently the lead is found in smaller particles and occurs in discrete droplets, even at grain edges (Fig 23). From being slightly harmful, lead becomes completely harmless. This is a result solely of its spatial distribution, which in turn must follow from the geometry imposed by the little triangle of forces established by surface tension wherever grain boundaries and phase interfaces meet.

The effect of bismuth in copper is an even more spectacular illustration of the significance of the dihedral angle of a liquid phase. Let us start with the lead-copper alloys mentioned above and add bismuth. To a first approximation, bismuth and lead can be regarded as being insoluble in copper at temperatures below  $900^\circ\text{C}$ , and the liquid to consist of lead and bismuth in the proportions added. Starting with the  $65^\circ$  triangles of lead, it is found that the dihedral angle becomes less as bismuth is added, the triangular prisms become sharper and sharper, until at somewhere above 75 pct bismuth, the angle becomes zero, the liquid spreads entirely around the grain boundaries, and the resulting metal is extremely brittle both hot and cold. This is clearly seen in the micrographs of alloys with 75 and 100 pct bismuth as the liquid phase (Fig 24 and 25). Experimental values of the angle, as determined in a series of rolled and annealed alloys, are shown in Fig 26. Distribution curves of the measured angles of two of these are given in Fig 27. The pure copper-bismuth alloy with lead was worked by compressing in a steel die for it could not be rolled sufficiently to produce recrystallization. One can ameliorate the brittleness in copper caused by bismuth by adding an equal quantity of lead—surely not a very promising addition from any other point of view than that of surface energy modification.

The dihedral angle is of great significance in connection with the penetration of a molten metal into a solid one of higher

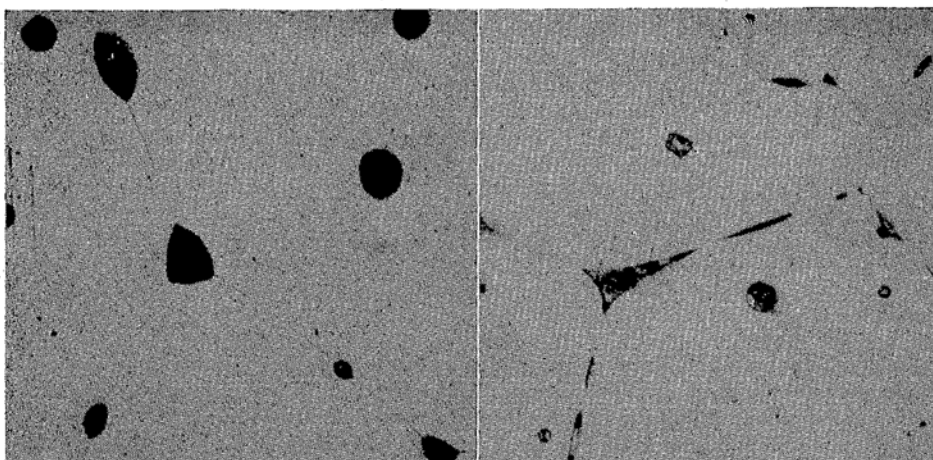


FIG 23

FIG 24

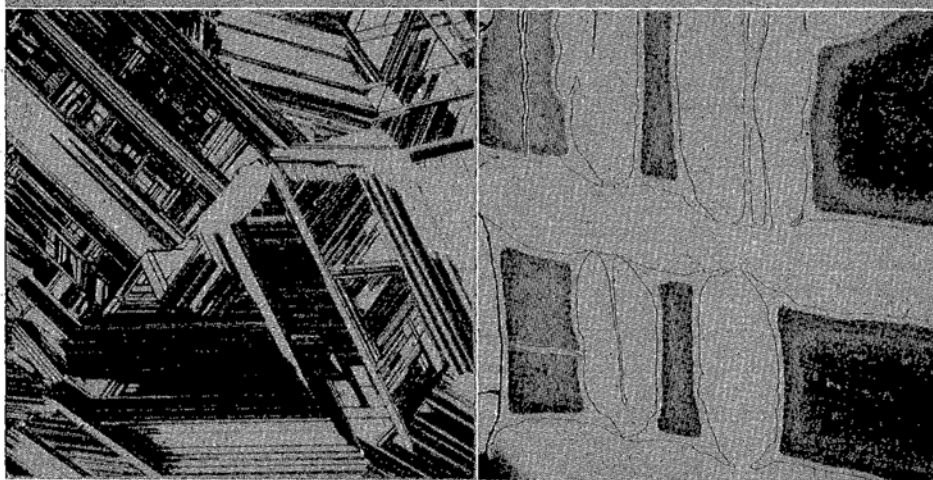


FIG 30

FIG 31

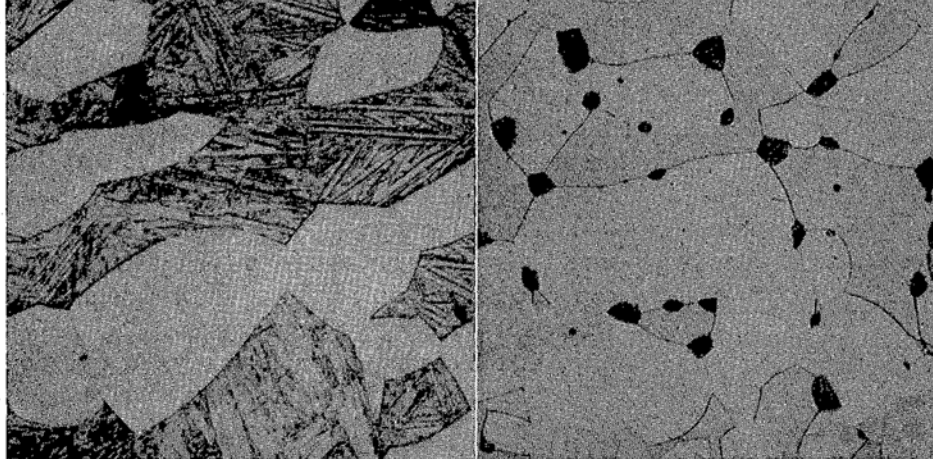


FIG 32

FIG 34

FIG 23—(843-1) BETA + LIQUID IN LEADED BRASS (51-46-3 Cu-Zn-Pb. ANNEALED 16 HR AT 700°C, QUENCHED. DICHROMATE ETCH.  $\times 250$ ).

FIG 24—(763-2A) LIQUID IN COPPER-BISMUTH-LEAD ALLOY (99- $\frac{3}{4}$ - $\frac{1}{4}$  Cu-Bi-Pb. ANNEALED 16 HR AT 750°C, QUENCHED. DICHROMATE ETCH.  $\times 500$ ).

FIG 30—(566-1) ALPHA + KAPPA COPPER-SILICON ALLOY. (95.6-5.4 Cu-Si. ANNEALED 1 HR AT 800°C, 1 MIN. AT 600°C, QUENCHED. ALKALINE PEROXIDE ETCH.  $\times 250$ ).

FIG 31—(136-20) CARLTON METEORITE, SHOWING TAENITE ( $\gamma$ ) PENETRATING BETWEEN GRAINS OF KAMACITE ( $\alpha$ ). (NITAL ETCH.  $\times 50$ ).

FIG 32—(1020-1) ALPHA-BETA ALUMINUM BRONZE (89.5-10.5 Cu-Al. ANNEALED 16 HR AT 650°C. DICHROMATE ETCH.  $\times 500$ ).

FIG 34—(795-1) THREE PHASE ALPHA-BETA-LIQUID STRUCTURE (79-17-4 Cu-Sn-Pb. ANNEALED 24 HR AT 600°C. PEROXIDE AND DICHROMATE ETCHES.  $\times 250$ ).

melting point. If the solid metal is slightly soluble in the liquid, it will commence to dissolve, being attacked most rapidly at the grain boundaries. If the dihedral angle is

of about  $65^\circ$ , while bismuth has penetrated between the grains and appears far below the surface, leaving thin films of extremely brittle material in place of sound bound-

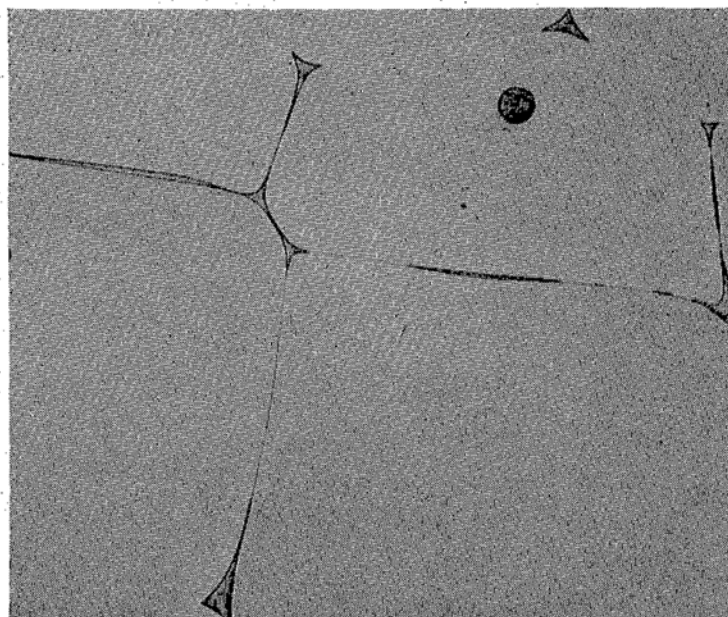


FIG 25—(1017-2) COPPER + LIQUID BISMUTH (99-1 Cu-Bi. PRESSED IN DIE, ANNEALED 16 HR AT 750°C. DICHROMATE ETCH.  $\times 250$ ).

greater than zero, penetration at the grain boundaries will stop as soon as the dihedral angle is reached and further solution must occur under conditions that will maintain this angle. However, if the dihedral angle is zero, penetration proceeds continuously along the grain boundaries and the liquid metal will be carried in by capillary action, prying apart the grains and eventually completely disintegrating the solid. This action can be accelerated by stress and it is probable that a tensile stress can cause penetration even when  $\theta$  is somewhat greater than zero. It should be noted that penetration will occur linearly along grain edges as long as  $\theta$  is below  $60^\circ$  and will spread progressively over the grain faces as  $\theta$  approaches zero.

Fig 28 and 29 show strikingly the difference between lead and bismuth in their action on the surface of polycrystalline copper. Lead has stopped its attack after opening up the grain boundaries to an angle

of about  $65^\circ$ , while bismuth has penetrated between the grains and appears far below the surface, leaving thin films of extremely brittle material in place of sound bound-

aries. If copper is heated in contact with bismuth, or even with bismuth vapor, it is rapidly rendered hopelessly brittle. Lead has no such effect and even if copper contains a small amount of lead it is not affected by being heated with bismuth, at least for reasonable annealing times.

It is apparent from Fig 26 that the ratio of interface and grain boundary tensions in the case of pure bismuth-copper is very near 0.5, and from Fig 4 it can be seen that near this value a small change of energy produces a large change in angle. Additions of phosphorus, zinc, oxygen, and probably many other elements, render bismuth-copper ductile by changing the dihedral angle. There has been some excellent work on this vexing and perplexing problem of bismuth in copper. Blazey<sup>4</sup> and particularly Voce and Hallowes<sup>5</sup> have described the phenomena in much detail, and Rhines<sup>6</sup> has suggested an explanation of the effect of heat treatment based on temperature-

dependence of the surface energy relations between the molten metal and the grain boundaries.

The amounts of bismuth needed to cause

rendered ductile by larger additions of phosphorus, contained the bismuth in the form of tiny triangles at the grain boundaries and not as films, exactly as required by

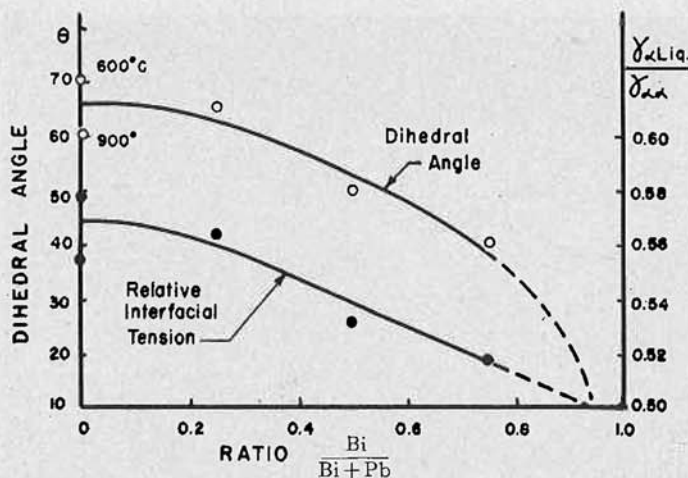


FIG. 26—DIHEDRAL ANGLE OF LIQUID PHASE IN COPPER-LEAD-BISMUTH ALLOYS AS A FUNCTION OF COMPOSITION.

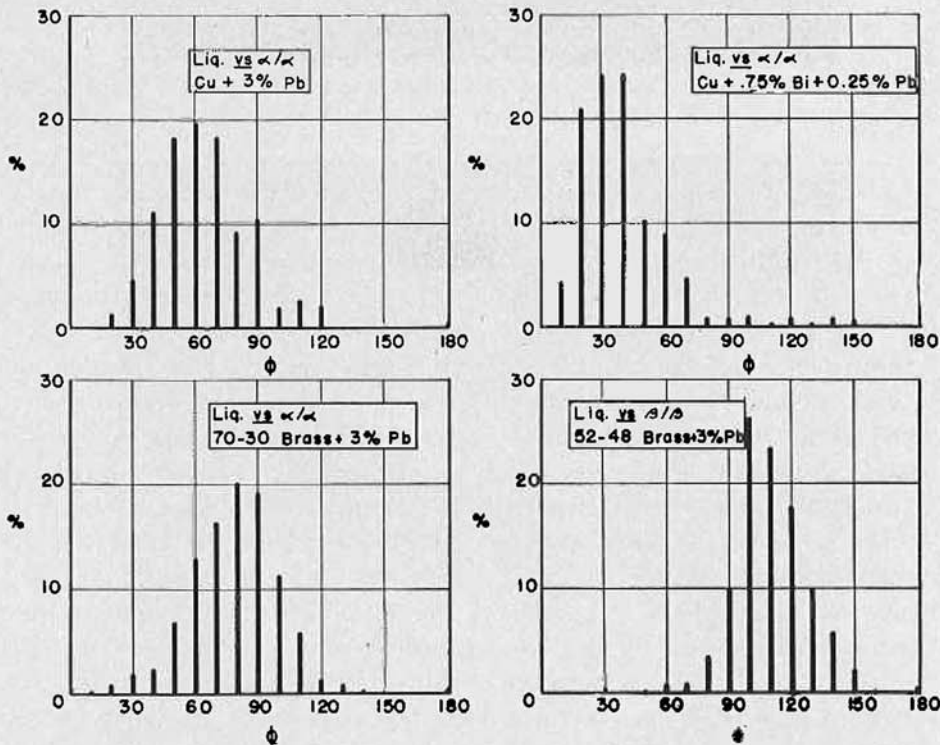


FIG. 27—DISTRIBUTION OF MEASURED ANGLES OF LIQUID PHASE IN MICROSECTIONS OF COPPER ALLOYS CONTAINING LEAD.

brittleness in copper are so small that microscopic identification is difficult; nevertheless, Schofield and Cuckow<sup>7</sup> did find grain boundary films in bismuth-embrittled copper and showed that such copper, when

the above theory. It should be noted that the phosphorus is not acting as a deoxidizer but is modifying the surface energy. It is a physical, not a chemical, effect.

In alpha-beta brass bismuth becomes

quite harmless, just as lead is when added to these brasses. Bismuth in alpha brass is far more tolerable than in copper and, if additions of phosphorus are also made, the

that given for the behavior of lead in the same brasses, although the dihedral angle at a given composition is smaller, and the difference more pronounced.

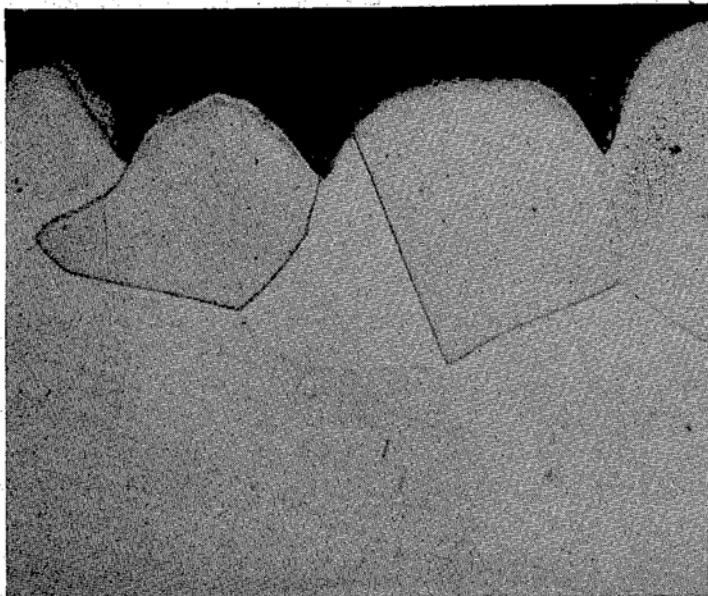


FIG 28—(806-1) SECTION THROUGH SURFACE OF COPPER HEATED IN CONTACT WITH LIQUID LEAD,  
24 HR AT 700°C. (DICHROMATE ETCH. X 500.)

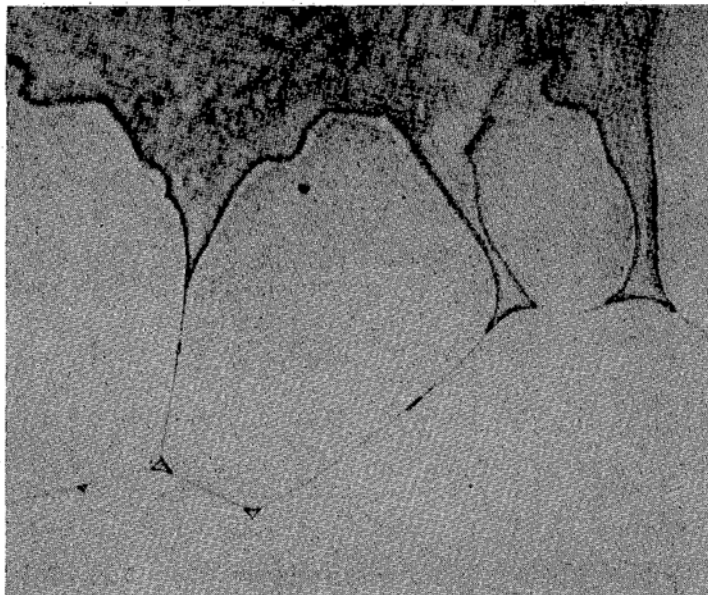


FIG 29—(807-1) SECTION THROUGH SURFACE OF COPPER HEATED IN CONTACT WITH LIQUID BISMUTH  
24 HR AT 700°C. (DICHROMATE ETCH. X 500.)

alloys become quite acceptable for all commercial use except hot working.<sup>8</sup> The explanation of these hitherto baffling effects in terms of dihedral angle parallels exactly

The amount of bismuth in otherwise pure copper that can be tolerated without producing brittleness increases with increasing annealing temperature, at least up to

800°C, where it is 0.01 pct.<sup>4,5</sup> That there is not—as suggested by Rhines<sup>6</sup>—a large change in relative surface energies with temperature was shown in the related case of lead in copper by measurements of the dihedral angle, which was between 50 and 65° (within experimental error) after annealing at temperatures of 600, 700, and 900°C. Indeed, one would rather expect a decrease in  $\theta$  with temperature in a system like bismuth-copper where the copper content of the liquid rapidly increases. Moreover, if such a change in angle were responsible for improvements on quenching from high temperatures, then the amount of bismuth tolerable should increase rather suddenly above a critical temperature. One is left, therefore, with a strong belief that *any* undissolved bismuth is harmful and that the increased toleration for bismuth on quenching from high temperatures is caused solely by increased solid solubility of bismuth in copper. Though in most alloy systems the solubility does not increase with increasing temperature when the second phase is a liquid, this is by no means impossible. Two cases are already well substantiated—silver-lead and copper-cadmium—and it is to be expected in many systems wherein the ratio between the concentrations of liquid and solid is large and where there is a large temperature interval between the solidus and liquidus.

Since the interface between solid bismuth and copper is probably of higher energy than that with liquid bismuth, it is unlikely that the equilibrium configuration of bismuth in copper below the eutectic temperature would cause brittleness. However, the rate of diffusion is so low at this temperature that no change in shape or distribution can occur in reasonable time. Actually, all alloys are in an extremely brittle state during solidification, and if most of them later become ductile it is only because diffusion and surface forces reshape the second phase subsequent to complete solidification. Very few alloys

containing a small amount of a brittle constituent are as brittle as bismuth copper. The difference between harmless and harmful impurities (when present in a molten condition or as a brittle solid phase) is entirely one of the relation between the interfacial tensions concerned, and the resulting angles of equilibrium with the grain boundary at the lowest temperature at which adjustment could occur.

When a eutectic occurs in small amount in an alloy its general effect on the mechanical properties will generally be greater if the composition of the eutectic itself is far removed from the primary constituent. The eutectic after solidification will then consist mainly of the second constituent. A "dilute" eutectic on solidification will cause further growth of the primary crystals and the minor phase generally has plenty of opportunity to spheroidize. Thus, while iron sulphide eutectic in steel is very harmful and leaves strings of virtually pure iron sulphide, copper sulphide in copper forms a relatively harmless eutectic consisting mostly of copper.

#### SOLIDIFICATION OF MOLTEN ALLOYS

There is an important corollary of the fact that the surface energy of a liquid/solid interface may be less than that of an intercrystalline grain boundary. During solidification and as long as even a trace of liquid is left, surface tension will insure that all surfaces of a crystal are wet. As fast as liquid freezes, more will be brought in by capillary action. Thus even though two growing crystals meet each other and consume all the liquid originally between them, growth will continue by capillary feeding to the interface which will eventually become a grain boundary. One grain will not cohere to another even under light pressure as long as liquid is present. The progressive drawing-in of liquid and its solidification will push the growing crystals away from each other until they abut in a manner to block each other rigidly; even then the boundaries

will stay wet, and the subsequent progressive solidification will occur under conditions that will locally fully satisfy surface tension requirements. It has heretofore seemed puzzling that the interior equiaxed portion of a metal ingot should have grains approximating the shape demanded by surface tension—quite different from that which would result from uniform growth from randomly occurring nuclei—but this is exactly what would happen as long as grain boundaries are continually wet by the liquid. Quincke<sup>9</sup> even postulated that a foam structure of a second phase occurred in the liquid; actually it is the liquid itself that forms the surface tension foam and isolates all solid crystals, with the same effect on the geometry as if there had been two liquids.

That crystals actually are pushed away from a wall and are free to fall or rise by gravity was conclusively shown by Watson.<sup>10</sup> Grains growing under a steep temperature gradient will, of course, be held near the mold wall and will grow in a columnar fashion until they meet the obstruction of interlocked grains growing from free nuclei. Further indication that the nuclei in the equiaxed portion really are free is to be found in the paper of Spretnak.<sup>11</sup> He observed an abrupt change in slope of the curve showing thickness of shell of a steel ingot retained on dumping as a function of square root of solidification time. This change occurred at the end of columnar crystal growth, and strongly suggests that central crystals in relatively large amount were being poured out with the liquid when the mold was dumped.

#### TWO-PHASE STRUCTURES IN SOLID ALLOYS

The interface energy between two different solid phases is generally more than half the energy associated with the grain boundary of either phase. Exceptions are the cases of exactly oriented interfaces between face-centered cubic and hexagonal structures of identical atom spacing [ $\alpha/\kappa$  copper silicon alloys, (Fig 30) and  $\alpha/\beta$  cobalt] and

possibly taenite and kamacite in meteorites (Fig 31), which have approached equilibrium at temperatures lower than those possible in any laboratory experiment. The majority of interphase energies in the solid are higher than intercrystal energies—hence the prevalence of two-phase structures consisting of approximately spheroidized particles—but many of the commercially important alloys lie in the range where the interphase energy is between 0.5 and 1.0 that of the grain boundary.

Let us consider the alpha-beta alloys of copper with tin, zinc, and aluminum, the microstructures of which have strong resemblance to each other. Photographs of typical structures are shown in Fig 10 to 13 and 32. Note that a grain boundary in either alpha or beta phase is invariably in conjunction with an apex on the grain of the other phase that adjoins it. The entire microstructure is (neglecting twins) a simple pattern made up of a network of grains bounded by short arcs intersecting in vertices three at a time. This is identical with the network in a single-phase polycrystalline material, but there is the important difference that the dihedral angle of  $120^\circ$  in single-phase material is replaced at three-grain two-phase contacts with one angle less than  $120^\circ$  and two angles more than this. Three grains of the same phase, regardless of which one, meet at the  $120^\circ$  angle. The vertex of a beta grain balanced by an alpha boundary has a different dihedral angle from an alpha grain abutting against a beta boundary, though both are less than  $120^\circ$ . The actual values of the angles in the cases of alpha-beta structures as well as some others are shown in Table 1. Some of the distribution curves on which these are based are given in Fig 33.

In the alpha-beta microstructures containing approximately equal amounts of the two phases the two-phase boundary is generally curved, and the boundary between two grains of the same phase is much straighter than usual in a single-phase

alloy. The alloy has solved the difficult integral equations and gives the minimum total surface energy; this clearly favors a smaller area and lower curvature of the high energy boundaries at the expense of the others.

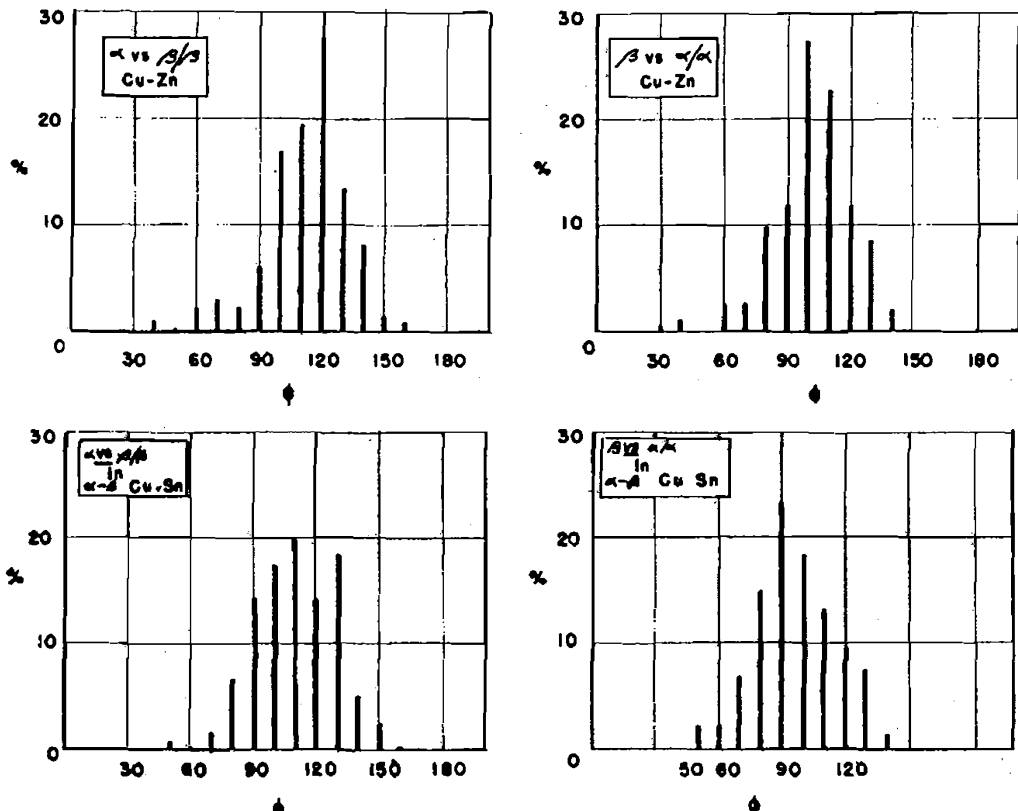


FIG. 33—FREQUENCY CURVES OF OBSERVED ANGLES OF MICROCONSTITUENTS IN ALPHA-BETA COPPER ALLOYS.

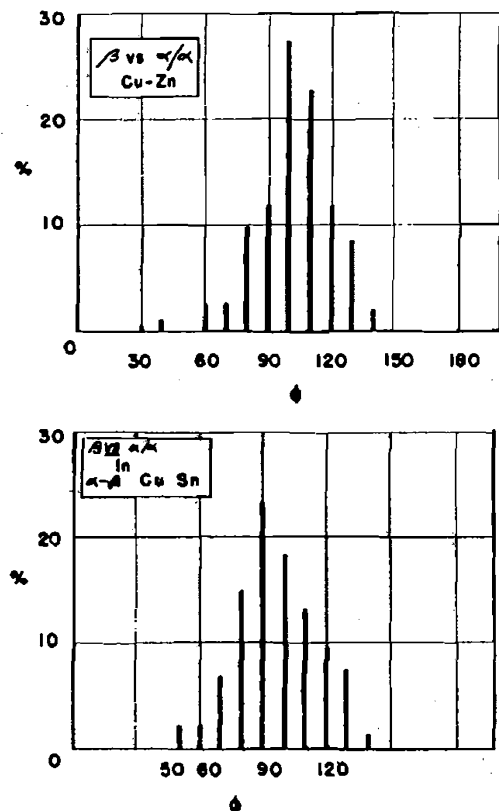
Because the beta vs. alpha/alpha dihedral angle is smaller than that of alpha vs. beta/beta, the characteristic "Gothic arch" structure is frequent for alpha grains, while beta where it abuts against alpha/alpha is like a section of a hollow-ground razor.

Since the beta and alpha dihedral angles in a brass, for example, are both obtained by equilibrium against the same alpha/beta interface, a quantitative ratio of the two grain boundary energies is obtainable. With  $\theta_\alpha = 115^\circ$  and  $\theta_\beta = 90^\circ$ , the interphase boundary ( $\gamma_{\alpha\beta}$ ) is, from Fig 4, 0.93 of the beta grain boundary ( $\gamma_{\beta\beta}$ ) and 0.71 of the alpha grain boundary ( $\gamma_{\alpha\alpha}$ ). The ratio of alpha to the beta boundary tensions is

therefore

$$\frac{\gamma_{\alpha\alpha}}{\gamma_{\beta\beta}} = \frac{0.93}{0.71} = 1.31.$$

The exact geometry depends upon the amount of the two phases, for the number



of single-phase and two-phase vertices and their spacings will depend on the relative amount of the two phases. Moreover, the whole structure will be affected by any deformation to which the piece may be subjected, and particularly if there are changes in solubility, by its entire thermal history.

Though in a section of a single-phase alloy a four ray vertex is rare (again omitting twins), it is more common in two-phase alloys. Two grains of beta form a boundary between themselves of higher energy than an alpha/beta interface when two grains of a phase are surrounded by two grains of the other; the grain boundary therefore will tend to decrease, and may eventually reach a point where the adjacent

alpha grains are brought in contact. Further movement in either direction would increase the area of one or other of the high-energy single phase grain boundaries,

quently partially replacing an alpha-alpha grain boundary, less frequently along a beta-beta grain boundary, and still less frequently associated with an alpha/beta

TABLE 2—Comparisons of Intersfacial Tensions in Three-phase Cu-Sn-Pb Alloy  
Specimen A-2133. 79/17/4 Cu-Sn-Pb. Hot rolled, annealed 4 hr at 750°C, furnace cooled to 600°C and held 24 hr at 600°C. Etched with potassium bichromate. Measured at 500X.

Observed Dihedral Angles, $\theta$	Ratio of Interface Tensions Derived from $\theta$	Computed Relative Interface Tensions		
		Interface	Relative Interface Tension	Based on Measured Angles No.
(1) $\alpha$ vs. $\beta/\beta = 120^\circ$	$\gamma_{\alpha\beta} = 1.00 \gamma_{\beta\beta}$	$\alpha\alpha$	1.35 1.31	2 3 and 5
(2) $\beta$ vs. $\alpha/\alpha = 95^\circ$	$\gamma_{\alpha\beta} = 0.740 \gamma_{\alpha\alpha}$	Average	1.33	
(3) Pb vs. $\alpha/\alpha = 90^\circ$	$\gamma_{\alpha Pb} = 0.707 \gamma_{\alpha\alpha}$	$\beta\beta$	1.00 1.05	1 4 and 5
(4) Pb vs. $\beta/\beta = 110^\circ$	$\gamma_{\beta Pb} = 0.872 \gamma_{\beta\beta}$	Average	1.03	
(5) Three-phase corner		$\alpha\beta$	1.00	Standard
(a) Pb vs. $\alpha/\beta = 110^\circ$		$\alpha Pb$	0.96 0.92	3 and 2 5
(b) $\beta$ vs. $\alpha/Pb = 120^\circ$	$\frac{\gamma_{\alpha\beta}}{\sin 110^\circ} = \frac{\gamma_{\alpha Pb}}{\sin 120^\circ} = \frac{\gamma_{\beta Pb}}{\sin 130^\circ}$	Average	0.94	
(c) $\alpha$ vs. $\beta/Pb = 130^\circ$	or $\frac{\gamma_{\alpha\beta}}{0.940} = \frac{\gamma_{\alpha Pb}}{0.866} = \frac{\gamma_{\beta Pb}}{0.766}$	$\beta Pb$	0.87 0.81	4 and 1 5
		Average	0.84	

hence the structure is in equilibrium with two grains of beta of different orientation meeting at a point with two grains of alpha, also different in orientation. Three-dimensionally the point becomes, of course, a line.

One sees, then, that the determining factor in equilibrium microstructures is the relation between the energy of the interface between crystal grains of one and the same composition and structure, and that between crystal grains of different composition and structure—that is, the relation between boundaries of a single-phase and two-phase nature.

### THREE-PHASE STRUCTURES

On introducing a third phase into a two-phase alloy and allowing the structure to reach equilibrium, the third phase will distribute itself in a manner to achieve the lowest total surface energy. Thus lead in alpha-beta bronze is to be found most fre-

boundary (Fig 34). The energies and resulting angles of the lead against the alpha and beta grain boundaries and of beta and alpha against the alpha-beta boundary are, of course, exactly the same as they would be in two phase alloys. In addition there are three phase corners with three interphase interfaces and no single-phase grain boundaries. By measuring the appropriate angles formed by the various combinations of interfaces, one can directly relate all the surface energies to each other and obtain quantitative values of their ratios just as in two-phase alloys, but with the added important possibility of determining the ratio of any two interface energies by two entirely independent routes. If the two values agree, it would be strong evidence that the angles really do result from equilibrium between surface forces.

The actual angle measurements made on the sample of leaded alpha-beta brass

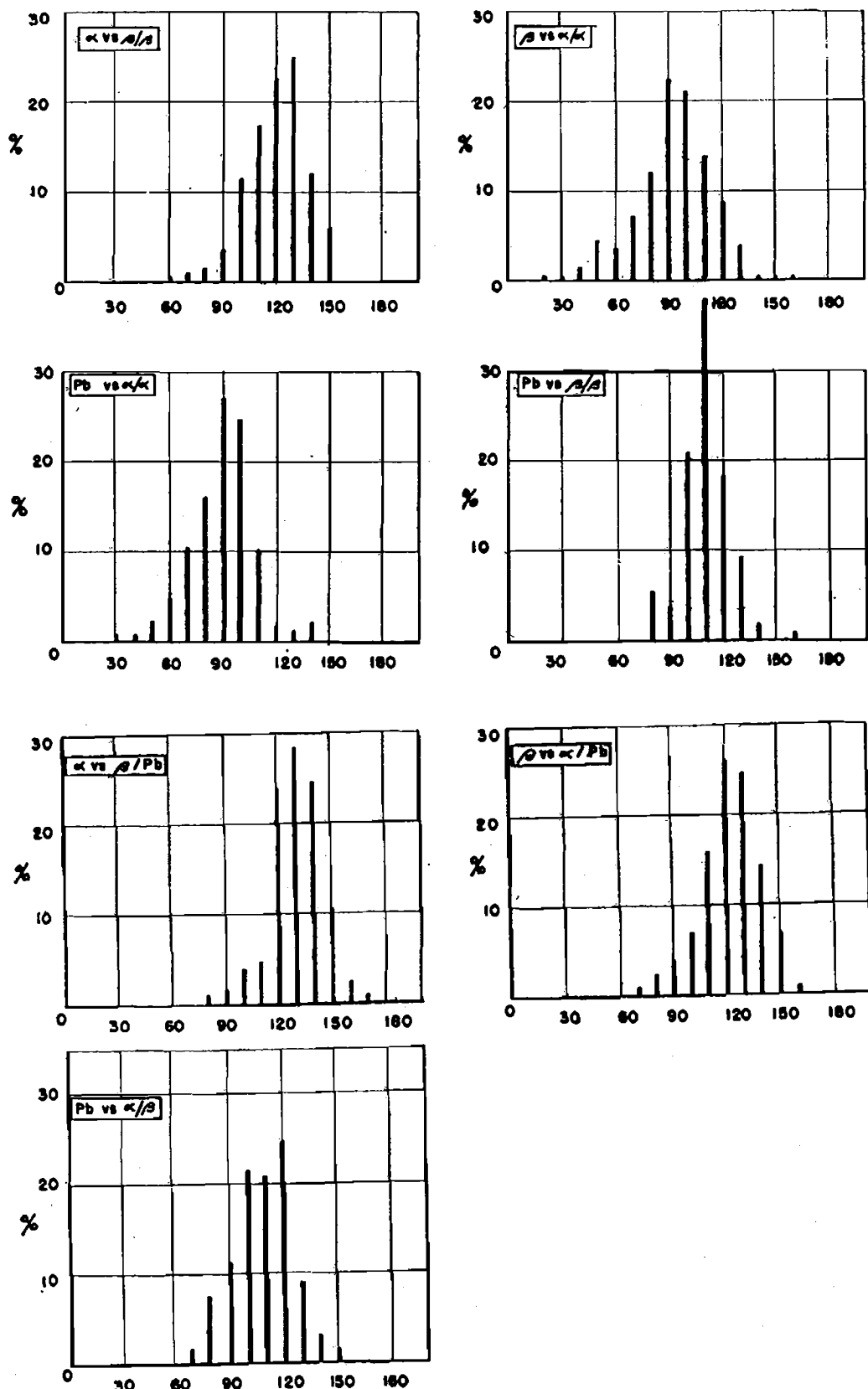


FIG 35—FREQUENCY CURVES OF OBSERVED ANGLES OF MICROCONSTITUENTS IN ALPHA-BETA-LEAD ALLOY (SEE FIG 34).

shown in Fig 34 are given in Fig 35. The dihedral angles derived therefrom are the basis of the calculations summarized in Table 2. The calculations in Column 4 were

quite independently for each of the interface energies are in reasonable agreement with each other. They may be made identical by adjusting the observed values by less

TABLE 3—Comparisons of Interfacial Tensions in Three-phase Zn-Cu-Al Alloy  
Specimen A-2104-A, 90/6/4 Zn-Cu-Al, hot rolled, annealed 48 hr at approximately 375°C.  
Microsample etched with chromic acid and sodium sulfate.

Observed Dihedral Angles, $\theta$	Ratio of Interface Tensions	Computed Relative Interfacial Tensions		
		Interface	Relative Interface Tension	Based on Measured Angles No.
(1) $\eta$ vs. $\epsilon/\epsilon = 115^\circ$	$\gamma_{\eta\epsilon} = 0.93\gamma_{\epsilon\epsilon}$	$\eta\eta$	1.00	Standard
(2) $\eta$ vs. $\beta/\beta = 120^\circ$	$\gamma_{\eta\beta} = 1.00\gamma_{\beta\beta}$	$\epsilon\epsilon$	1.00	1 and 3
(3) $\epsilon$ vs. $\eta/\eta = 115^\circ$	$\gamma_{\eta\epsilon} = 0.93\gamma_{\eta\eta}$	$\eta\eta$	1.02	6, 4, 2, and 5
(4) $\epsilon$ vs. $\beta/\beta = 110^\circ$	$\gamma_{\epsilon\beta} = 0.87\gamma_{\beta\beta}$	$\beta\beta$	Average 1.01	
(5) $\beta$ vs. $\eta/\eta = 110^\circ$	$\gamma_{\eta\beta} = 0.87\gamma_{\eta\eta}$		0.87	2 and 5
(6) $\beta$ vs. $\epsilon/\epsilon = 95^\circ$	$\gamma_{\epsilon\beta} = 0.74\gamma_{\epsilon\epsilon}$		0.85	4, 6, 1 and 3
			Average 0.86	
		$\eta\epsilon$	0.93 0.95	1, 6, 4, 2, and 5
		$\epsilon\beta$	Average 0.94	
			0.74 0.76	6, 1, and 3 4, 2, and 5
		$\beta\eta$	Average 0.75	
			0.87 0.85	2, 4, 6, 1, and 3
			Average 0.86	

done in the following manner, using  $\gamma_{\alpha\beta} = 1.0$  as the standard for intercomparison.

$$\gamma_{\alpha\alpha} = \frac{\gamma_{\alpha\beta}}{0.74} = 1.35$$

directly from Eq 2 in Table 2. Alternatively, however, from Eq 3,

$$\gamma_{\alpha\alpha} = \frac{\gamma_{\alpha Pb}}{0.707}$$

and, from Eq 5,

$$\gamma_{\alpha Pb} = \frac{0.866}{0.940} \gamma_{\alpha\beta}.$$

Therefore

$$\gamma_{\alpha\alpha} = \frac{0.866}{0.940 \times 0.707} = 1.31.$$

The other values are computed in an analogous manner. The two values obtained

than  $5^\circ$ . One can surely conclude, therefore, that microstructures are not fortuitous, but that the surfaces arrange themselves as they must under the reaction of the various surfaces seeking to establish a minimum value of total energy.

We now see the reason for the particular distribution of lead observed in the structure in Fig 34. Although the alpha-beta interface is of nearly the same energy as the beta-beta boundary, lead drops are rarely found on the former for the difference between the alpha-beta interface and the alpha-lead and beta-lead boundaries that replace it when a lead drop occurs at this point is less than if the lead replaces either an alpha-alpha or a beta-beta boundary ( $\gamma_{\alpha\alpha} - \gamma_{\alpha Pb} = 0.39$ ;  $\gamma_{\beta\beta} - \gamma_{\beta Pb} = 0.29$ ; and  $\gamma_{\alpha\beta} - \frac{\gamma_{\alpha Pb} + \gamma_{\beta Pb}}{2} = 0.11$ ).

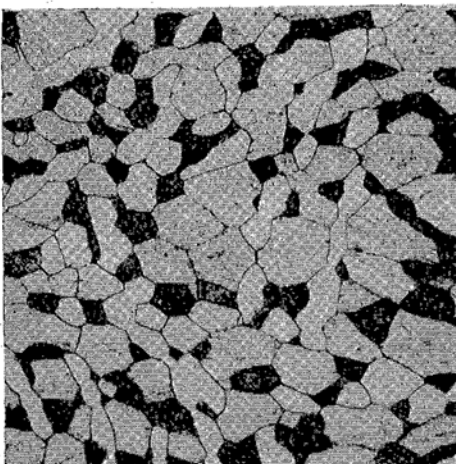


FIG 36



FIG 38

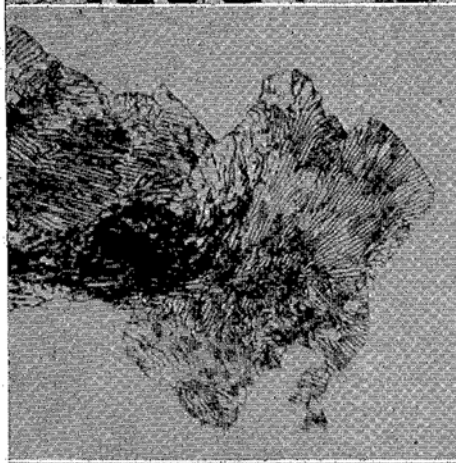


FIG 39



FIG 40

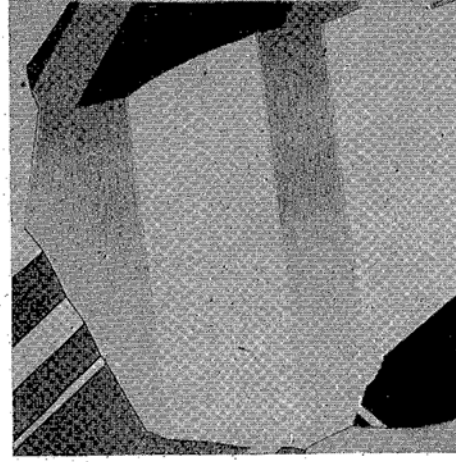


FIG 45

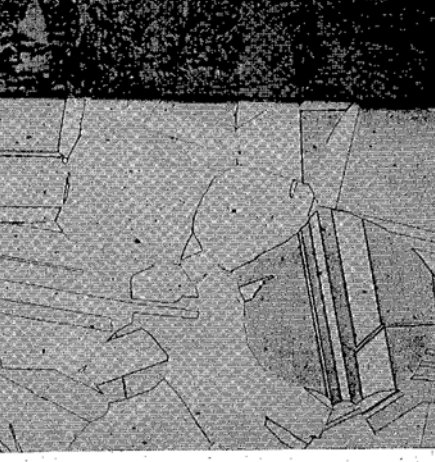


FIG 47

FIG 36—(1008-1) THREE-PHASE ZINC-COPPER-ALUMINUM ALLOY (90-6-4 Zn-Cu-Al. ANNEALED 48 HR AT 370°C. SPECIAL CHROMIC ACID ETCHES.  $\times 500$ .)

FIG 38—(852-3) EUTECTOID NODULE GROWING ISOTHERMALLY IN BETA ALUMINUM BRONZE AT 545°C. (DICHROMATE ETCH.  $\times 500$ .)

FIG 39—(886-1) PEARLITE NODULE GROWING ISOTHERMALLY IN S.A.E. 1085 STEEL AT 690°C. (NITAL ETCH.  $\times 1000$ .)

FIG 40—(879-2) DISCONTINUOUS PRECIPITATION IN BERYLLIUM COPPER (98-2 Cu-Be. QUENCHED FROM 825°C, REHEATED 4 HR AT 450°C. DICHROMATE ETCH.  $\times 1000$ .)

FIG 45—(593P-4) JUNCTION OF TWIN AND GRAIN BOUNDARIES IN 70-30 BRASS. (ANNEALED 1 HR AT 700°C. AMMONIA AND PEROXIDE ETCH.  $\times 75$ .)

FIG 47—(1021-1) JUNCTION OF GRAIN BOUNDARIES WITH FREE SURFACE OF ALPHA BRASS.

Note that grain boundaries join the surface nearly perpendicularly. (70-30 brass annealed 24 hrs. at 650°C. Surface metallographically polished before annealing; copperplated thereafter and transversely sectioned. See Fig 43. Ammonia and peroxide etch.  $\times 100$ .)

As another example of the relation of the six possible interface energies in a three-phase alloy, consider Fig. 36, a Zn-Cu-Al alloy not far from the compositions used in die castings. There are approximately equal quantities of three phases— $\eta$  and  $\epsilon$  as in the copper-zinc system, and  $\beta$  (or  $\beta_1$ ) as in the aluminum-zinc system, all with small amounts of the third element in solid solution. It is easy to find any combination of phase corners for measurement. The angles and the calculated values of the various interfaces in terms of the energy of the grain boundary between two grains of zinc-rich solid solution are given in Table 3. The calculations were made as in the following example:

Using as a basis

$$\gamma_{\eta\eta} = 1.00 \text{ arbitrary units,}$$

from (3)

$$\gamma_{\eta\epsilon} = 0.93 \quad \gamma_{\eta\beta} = 0.93.$$

This can be calculated also by an entirely independent route, as follows:

from (1),

$$\gamma_{\eta\epsilon} = 0.93 \gamma_{\epsilon\epsilon}$$

from (1) and (6)

$$= 0.93 \frac{\gamma_{\epsilon\beta}}{0.74}$$

from (1), (6) and (4)

$$= \frac{0.93}{0.73} 0.87 \gamma_{\beta\beta}$$

from (1), (6), (4) and (2)

$$= \frac{0.93 \times 0.87}{0.73}$$

$$\times \frac{\gamma_{\beta\beta}}{1.00}$$

$$\text{from (1), (6), (4), (2), (5)} = \frac{0.93 \times 0.87}{0.73}$$

$$\times 0.87 \gamma_{\eta\eta}$$

$$= 0.95.$$

The other interface values are obtained each by two routes, using the groups of angle measurements shown in the table, and performing the calculations in the same way as in the example given with  $\gamma_{\eta\epsilon}$ . The good agreement of the two independent values again confirms the general validity of the concepts used.

In an alloy with four or more phases the same principles will apply. There will be equilibrium at the appropriate angle whenever three interfaces meet. A fourth grain (of whatever phase) appearing at a three-grain corner will establish the correct dihedral angle with each interface. Because of the existence of common sides to the various triangles of force, the angles between three interfaces are not disturbed by the introduction between them of a fourth grain; if extrapolated within the new grain, all the interfaces must intersect at a point at the correct angles.

In a four-phase alloy there is a possibility of four phases meeting along a common grain edge. This could occur whenever displacement would expose a fifth interface of higher interfacial tension than the four already meeting in equilibrium.

#### EFFECT OF SURFACE ENERGY ON TRANSFORMATION STRUCTURES

Throughout the above discussion it has been assumed that the two or more phases coexisted in compositional equilibrium and that the structures were produced by the migration of the grain and phase boundaries to reach geometric equilibrium of surface forces. When an alloy is not in equilibrium, as for example when undergoing precipitation or transformation, surface energy is of paramount importance in determining whether a nucleus can grow or not, but the elastic strain energy generally causes the interfaces to be those on which lattice matching can most easily occur. These are determined by lattice geometry and spacing, and the interfaces are not free to adjust themselves according to the principles outlined above, which assume that the energy is independent of the orientation of the interface. Thus in normal precipitation, Widmanstatten structure and orientation relationship exist at the early stages, though incoherence occurs when the particles reach sufficient size, and after extremely long annealing the plates

and rods of precipitate will generally yield to surface forces and spheroidize.

The case of a eutectoid transformation is quite different from precipitation. The

unbalanced. The short plate, *A*, would be accelerated in growth, *B* would be retarded, while *C* is subject to forces tending to deflect it as it grows. The forces probably

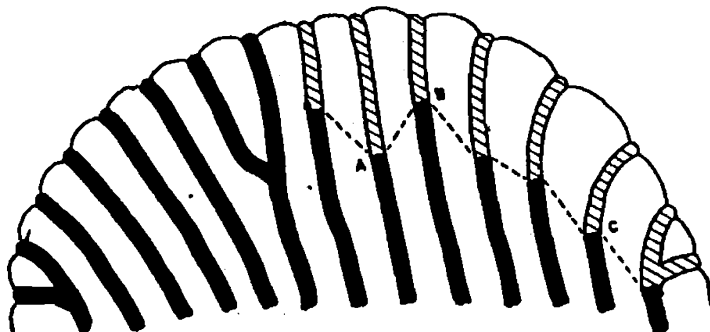


FIG 37—GROWTH OF EUTECTOID COLONY (SCHEMATIC).

interface between the eutectic or eutectoid nodule and the parent phase is incoherent; it is essentially a grain boundary, and the little triangle of forces will produce varying effects, depending on the relative values of the three interfacial tensions.

Let us consider, as an example, the  $A_1$  transformation in steel. A possible mechanism for the first stage would be the formation of a small plate of cementite at an austenite grain boundary followed by the parallel formation of a plate of ferrite, which breaks up into fingers under the influence of surface tension, starting from the periphery and exposing lines of cementite.\* Along the lines where three phases meet, each phase will have the dihedral angle required by the balance of surface energies and this will be maintained throughout subsequent growth. If the boundary between the austenite and the transformation products were plane, it would advance uniformly and the spacing would stay the same and the plates parallel. If surface forces are taken into consideration, this cannot be the case. In the example sketched in Fig 37, if the interface had by chance reached a position such as shown by the dotted line, the surface tensions at a three-phase junction would be completely

do not actually deflect the interfaces already formed, but an incorrect curvature will influence the transfer of atoms to or from a surface and thus modify the relative rates of growth until a proper balance is obtained. The surface shown by the solid outline is in approximate local equilibrium as far as surface forces are concerned. The interface tensions tend continually to deflect the advance of the cementite plates at the sides of the mass into a direction normal to the average surface at this point. The actual spacing is, of course, dependent on the speed of growth, diffusion, available free energy and total surface energy as shown by Zener.<sup>10</sup> As the spacing between the plates increases on continued growth there will be an increased chance of an accidental protuberance growing into the region of higher carbon content and, continually advancing, to become a stable branch. The microstructures of partly grown pearlite nodules in steel and in aluminum bronze (Fig 38 and 39, respectively) are consistent with this picture. The occasional appearance of plates nearly parallel to the boundary is probably a result of the random sectioning.

This mechanism allows a reasonable degree of interdependence of orientation between the various phases (for there are some orienting forces acting across even an essentially incoherent boundary) and allows

\* Some eutectoid constituents grow as rods, rather than plates, but the following conclusions will apply equally well to this case.

both phases to be continuous and of uniform orientation throughout a given colony. The exact shape of the two final constituents is found to depend, however, on the simple geometry required by the angles at the advancing interface between the parent phase and the two new ones. Any accidental local circumstance changing the interface energy between austenite and either of the other two phases would result in changing the direction of advance of the boundary. This could be an inclusion, or a local fluctuation of strain or composition. Crystallographic forces are not of primary significance, and idiomorphic crystals or Widmanstatten structures are rarely seen. Each plate would directly influence and be influenced by its neighbors, and all will tend to be set normal to the grain boundary of the nodule.

There are not necessarily three different phases involved in the three grains concerned with pearlitic growth. The three crystals may even be of the same phase differing only in orientation, the effective interface then being a grain boundary. The boundary adjacent to a strained lattice will probably have lower energy than with a perfect lattice, enabling two unstrained grains to grow into a strained matrix in recrystallization in a manner somewhat analogous to a eutectoid. Certainly the analogy is very close when two phases are involved, one of them being represented by two crystals of different orientation. This is actually the well-known case of discontinuous precipitation. As Gayler<sup>13</sup> has shown, discontinuous precipitation occurs when the decomposing solid solution is greatly supersaturated—supposedly because the change in parameter accompanying the process is large enough to render extensive coherency of the lattices impossible. It has been observed by Gayler, as well as by the writer,<sup>14</sup> Burke,<sup>15</sup> and others, that discontinuous precipitation is accompanied by recrystallization of the matrix. On appropriate etching, usually there can be seen

a perfectly normal-looking grain boundary defining the area in which precipitation has occurred. There is a sudden change in composition associated with such precipitation, which is nothing but a reaction occurring by local diffusion at an advancing front that is identical, as far as the surface forces are concerned, with that delineating a growing eutectoid colony. The alloy ahead of the boundary is unchanged except for local composition gradients; the area behind it consists of two phases in equilibrium, growing edgewise in coordination at the boundary. In many alloys the process is competitive with continuous precipitation in which many nuclei, different in composition from the matrix, will be growing with a low-energy coherent interface. This second "phase" may grow, with gradual depletion of the parent lattice, until at some time supersaturation of the latter is no longer sufficient to maintain incoherence with the equilibrium matrix of the same phase growing in the nodule of discontinuous precipitation. The nodule will then cease growing. Excellent examples of this are found in aluminum-magnesium alloys<sup>16</sup> and at both ends of the silver-copper system (see Gayler<sup>13</sup> and Smith and Lindlief<sup>17</sup>). Fig 40 shows similar behavior in the case of beryllium-copper alloys (a well-known example) and Fig 41 shows partial pearlitic precipitation in an alloy of zinc with 2 pct copper. In the latter sample continuous precipitation and long overaging have given rise to a well defined Widmanstatten pattern in those areas not consumed by the pearlitic growth. In beryllium-copper the "pearlite" grows into continuously precipitated areas even after long overaging; this could not happen if the particles were of approximately the same size and solubility as those growing in the pearlitic areas.

Another interesting example is found in the copper-aluminum system. Beta gives a normal eutectoid structure of alpha and gamma on holding just below its transfor-

mation temperature. If it is rapidly cooled to below  $385^{\circ}\text{C}$  it undergoes a diffusionless transformation to a form of martensite. As

martensite. If one chooses to call martensite supersaturated alpha, this is another case of discontinuous precipitation—



FIG 41

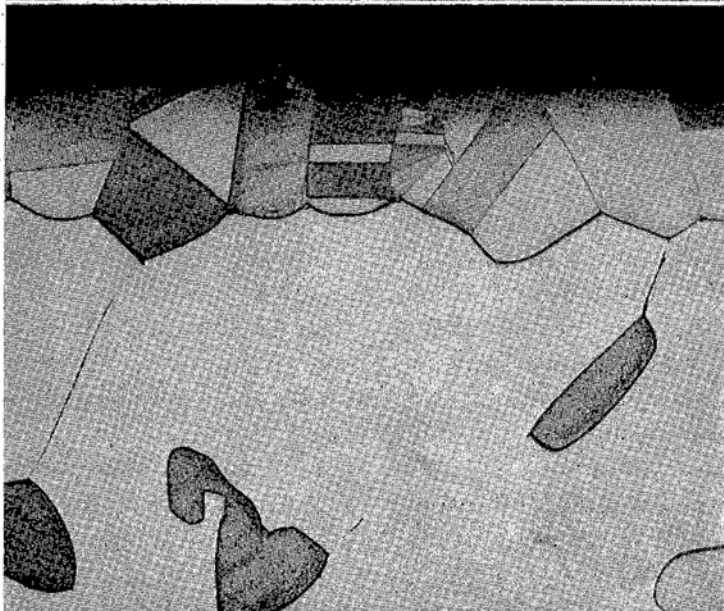


FIG 42

FIG 41—(883-1) PEARLITIC AND WIDMANSTÄTTEN PRECIPITATION COMPETING IN ZINC COPPER ALLOY (98-2 ZN-CU). ANNEALED 24 HR AT  $400^{\circ}\text{C}$ , REHEATED 24 HR AT  $250^{\circ}\text{C}$ . PALMERTON ETCH.  $\times 500$ .

FIG 42—(882-1) JUNCTION OF TWO PHASES FORMED BY DIFFUSION: DEZINCIFIED SURFACE OF ALPHA-BETA BRASS (60-40 CU-ZN). ANNEALED IN AIR, 24 HR AT  $650^{\circ}\text{C}$ . AMMONIA AND PEROXIDE ETCHES.  $\times 150$ .

Mack<sup>18</sup> has shown, if such quenched alloys are annealed for prolonged periods at about  $375^{\circ}\text{C}$ , a pearlitic structure appears, obviously growing at the expense of the

edgewise growth of equilibrium alpha and gamma phases with their interfaces in local equilibrium at a boundary advancing into the martensite. The spacing of the resultant

alpha plus gamma is larger than it would be had they transformed directly from beta at the same temperature, for the available free energy is less. Otherwise, the structure is very similar.

A freshly formed eutectoid structure will consist of plates or rods of one constituent in a matrix of the other. Both phases will be in continuous crystals of the same orientation throughout a single colony. Because there are no grain boundaries in either phase, except at the colony boundary, the phase in smallest amount will tend to spheroidize. Because a plate is unstable only at the edges, while a rod is unstable whenever its length exceeds its diameter, a rod will spheroidize more rapidly. Spheroidization may occur even in the first parts to form while the colony is still growing, giving rise to a discontinuous structure. The eutectic or eutectoid structure does not result from discontinuous or alternate crystallization of the two phases.

While continuous precipitation would tend to be crystallographically orientated, discontinuous precipitation, like eutectoidal decomposition, is not so shaped. Thus platelets deposited by continuous precipitation should show a typical Widmanstatten structure with changes of direction at twin boundaries in the matrix, while those resulting from discontinuous precipitation, like those resulting from eutectoidal transformation, should ignore twins, and be sensitive only to grain boundaries. It is well known that pearlite in steel shows no influence of the austenite twins.

If a particle of a precipitate forms at a grain boundary but grows into the body of the grain at an angle determined by strong orientation relationships, it may cause the grain boundary to follow it. This seems to be the reason for the jagged grain boundaries that are often observed in magnesium alloys on air cooling.<sup>16</sup>

The interface between two phases formed by gross diffusion from a plane surface will

also be affected by the surface forces. It will not be plane, but will consist of a series of more or less curved faces joining the pointed apices formed wherever a grain boundary in either phase meets the interphase boundary (Fig 42). The dihedral angle will, of course, be the same as in a grossly uniform alloy containing the same two phases.

#### DEPENDENCE OF GRAIN BOUNDARY ENERGY ON ORIENTATION DIFFERENCE

As Desch<sup>19</sup> and others have shown, the geometry of the network of grain boundaries in single phase metals and alloys does not differ greatly from that of a froth of soap bubbles. Thompson,<sup>20</sup> Lewis,<sup>21</sup> Matzke,<sup>22</sup> and others have shown that the cells in animal and vegetable tissue are also similar in many respects. Lewis shows drawings of cells in both elder pith and human fat that a metallurgist would immediately accept as sketches of isolated metal grains. In all three cases we are concerned with a similar system of forces and the geometry results from the attempt to achieve minimum surface energy from the various intersecting and interacting surfaces.

The fact that drops of liquid within single metal grains, as in Fig 17, are generally very close to spherical indicates that the crystal/liquid interfacial tension does not vary much with orientation, at least in the case of metals of cubic structure. The lack of sudden changes of direction at grain boundaries in the typical annealed metal shows that these, too, cannot be highly sensitive to orientation changes. There is, however, some effect of orientation and a quantitative study of it will prove to be a most powerful touchstone in determining the validity of various theories of the grain boundary.

The spread of dihedral angles around  $120^\circ$  is relatively large even with two-dimensional grains grown entirely through the specimen, so that the true intersection is normal to the surface studied (see the frequency curves of Fig 43A). A random

section through a three dimensional sample also shows greater than the theoretical spread of measured angles for  $\theta = 120^\circ$  (compare Fig 6 and 43B).

boundaries does disclose a number of twin/boundary intersections where the boundary slightly but sharply changes its direction. There are equal numbers of angles greater

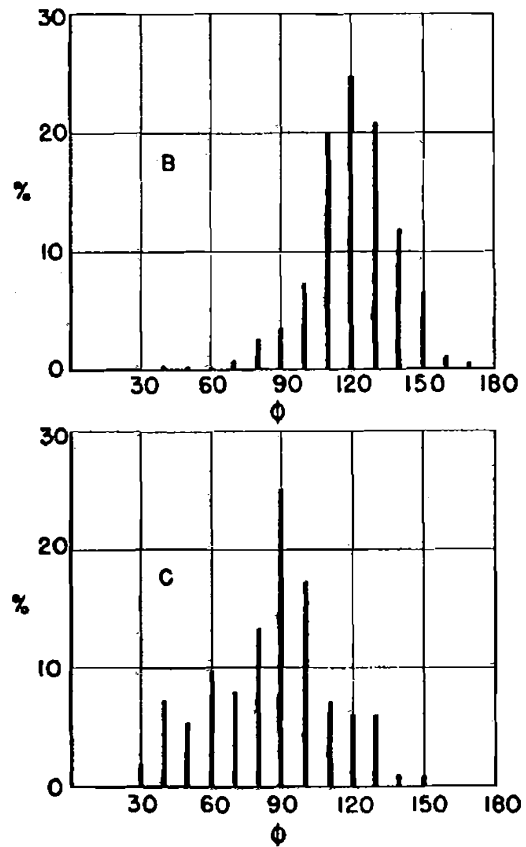
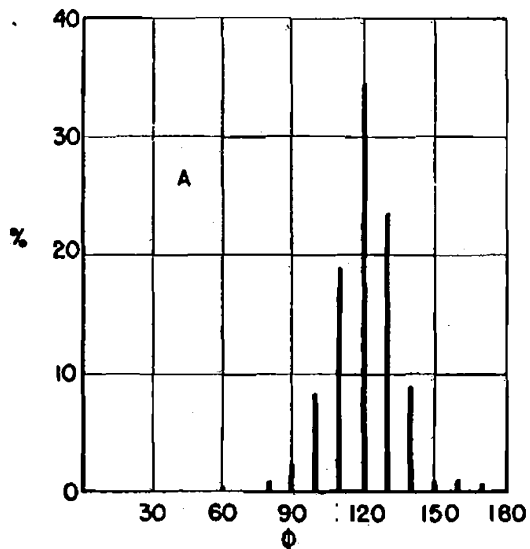


FIG 43—FREQUENCY OF OBSERVED ANGLES AT GRAIN CORNERS IN SINGLE-PHASE ALPHA BRASS.  
A = GRAIN CORNER ANGLES MEASURED PARALLEL TO THE SURFACE IN A THIN SHEET (0.1 MM THICK, 0.12 MM GRAIN SIZE); B = DISTRIBUTION IN RANDOM SECTION THROUGH CENTER OF SAMPLE (0.15 MM GRAIN SIZE, 5 MM THICK); C = INCLINATION OF BOUNDARIES AT POINTS WHERE THEY JOIN THE SURFACE.

The extremely small energy of the twin boundary in annealed face-centered cubic metals in relation to the grain boundary is deduced from the fact that a twin can meet a grain boundary at virtually any angle without much deviation of the latter. Were the twin to have even as little as one tenth the grain boundary energy, the junction would appear as at *a* in Fig 44, the angle between the two branches in the grain boundary there being  $174^\circ$ . This structure never occurs in metals that have annealing twins; indeed such a structure is obviously unstable, for the twins would be drawn together without hindrance and would disappear. However, inspection of grain

and less than  $180^\circ$ , as illustrated in the micrograph, Fig 45, and diagrammatically at *b* in Fig 44. If we persist in applying the concept of a local triangle of forces between the interface tensions, the energy in the twin boundary in some of the junctions is negative, corresponding to a surface compression, which is clearly impossible. The difficulty is resolved, however, if we take the twin boundary itself to be of negligible energy but assume the grain boundary tension to vary slightly and smoothly with the orientations of the adjacent grains, perhaps in some such manner as in Fig 46. A boundary will then deviate slightly from the minimum-area position between

the grain edges concerned in order to approach the direction of minimum energy. It will show slight preference for certain directions, though this will not be notice-

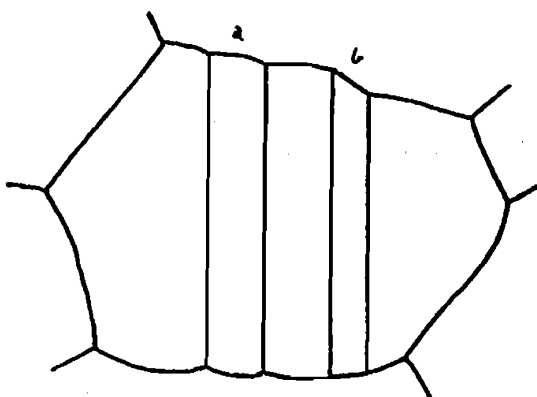


FIG 44—HYPOTHETICAL FORMS OF JUNCTION OF TWIN BOUNDARIES WITH THE GRAIN BOUNDARY.

able without careful measurements unless there is a discontinuity in the curve of energy vs. grain boundary direction for a pair of grains of fixed orientation difference. At those points where a twin in one grain joins the boundary there is a sudden change in grain alignment and the energy of the boundary does change discontinuously, for example, from *a* to *b* in Fig 43. There are forces deflecting the boundary in opposite directions on the two sides of the twin; the total energy is therefore less if the grain boundary adopts the zigzag course observed.

This effect, small though it is, is actually of importance, for it is responsible for the very existence of annealing twins. If it did not exist, the twin boundaries would either stay where they were first formed until the boundary of a growing grain encountered and engulfed them, or the twins would disappear under the influence of their own surface tension. The latter behavior is actually observed on annealing most metals that form deformation twins, for example, iron, zinc, and magnesium. A normal annealing twin that has once formed must lengthen with the movement of the boundary that it joins, otherwise it would

form a new interface of high energy. It is also easy for a twin to grow in a direction normal to the twinning plane if its edges become unstable. If, as in Fig 44, the twin

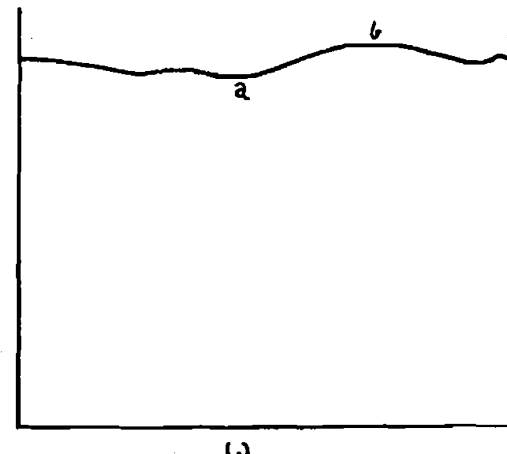


FIG 46—HYPOTHETICAL VARIATION OF SURFACE TENSION WITH ORIENTATION OF A GRAIN BOUNDARY BETWEEN TWO GRAINS OF FIXED ORIENTATION NOT IN TWIN RELATIONSHIP.

exposes a high energy face at the grain boundary, the twin boundary will be drawn in a direction to decrease the area of this surface. The twin, however, must maintain a plane surface and it is unlikely that it can continue to move transversely until it disappears at the side of the grain for it cuts many other faces of the grain and will establish a position of equilibrium where the total energy of all the faces concerned is a minimum. Because of the abrupt change in energy on moving from one face of a grain to another, there will be a tendency for twins to be associated with grain edges, more closely so as the directions of the twin and edge approach each other. As grain faces and edges move during growth, the twins must move with them. It is well known that approximately the same number of twins per grain and the same general geometry are maintained in large grains as in small ones, a fact that certainly suggests a mechanism such as the above where boundaries and twins grow proportionately together. If this view is correct, a spherical grain should have no mechanism for keeping its twins. The twin

frequency is actually observed to be less in materials which have been annealed above the solidus to surround the grains by liquid and remove their sharp edges, as well as in annealed brasses of high zinc content where small grains of the alpha phase are entirely surrounded by large grains of beta phase, without grain boundaries.

### GRAIN GROWTH

Let us consider the role of surface tension in grain growth in single phase alloys. The geometry of grain boundaries in a polycrystalline metal is similar to that of a mass of soap bubbles. In both cases there is inherent instability introduced by the curvatures that are necessary to reconcile the edge and corner angles with the number of lines and points of contact in a random assembly of grains. This leads to growth whenever there is a mechanism whereby surfaces that are not plane can move toward their center of curvature. This was suggested by Harker and Parker,<sup>3</sup> although their model needs some amplification. They believed that a stack of rhombic or trapezoidal dodecahedra met their specifications for a stable shape: Actually only eight of the fourteen vertices of a dodecahedron are correct, and at the other six vertices there are six cells and twelve boundaries meeting at a point in the stack, a condition of manifest instability. The only truly stable shape of grain is the minimum-area tetrakaidecahedron (cube-octahedron) of Lord Kelvin.<sup>23</sup> This has six plane four-sided faces and eight doubly-curved hexagons of zero mean curvature. There are 36 edges of equal length (all curved) and 24 vertices, at each of which three edges meet. It will fill space on a body-centered-cubic packing. Four cells meet at each vertex and the angles everywhere meet the surface tension requirements. A cross-section through a stack of such stable grains would *not* show all boundaries as straight lines. It is the mean curvature  $1/r_1 + 1/r_2$ , where  $r_1$  and  $r_2$  are

the radii measured at right angles to each other at any point in the surface) that is significant in grain growth, not the apparent curvature in any one plane.

Growth of bubbles in a froth is a result of the diffusion of gas through the walls of the smaller, more convex, high-pressure bubbles into their neighbors. This causes gradual readjustment until two adjacent faces are brought in contact at an unstable angle, whereupon there is rapid readjustment of the boundaries to conform to the new requirements. Growth in such a froth, and grain growth in metals, is a highly discontinuous process, not a continuous one. In a soap froth the ideal structure from which no further growth will occur cannot be achieved unless the boundary of the mass has fixed ridges of the correct geometry to anchor the films in conformation to the ideal geometry of the uniform-sized tetrakaidecahedra. An incorrect number of edges to just one face of any one of the polyhedra renders the whole structure unstable and movement will continue until the froth has been replaced by a few flat films between available boundary points.

It is obvious from the discussion in the earlier part of the paper that an inclusion, particularly one of low dihedral angle, will tend to become attached to a grain boundary. If the inclusion is rigid and insoluble, it will effectively anchor the boundary locally. If a moving boundary encounters such a particle, it will locally cling to it, causing a dimple in the surface, until the motion elsewhere has proceeded sufficiently far to cause it to break away. If there is a sufficient number of particles, even a strongly curved boundary will be unable to move and it is easy to see that there must exist a definite relation between the number and size of inclusions and the minimum curvature that can move. Clarence Zener<sup>24</sup> has treated this concept semiquantitatively in the following manner.

The driving force for grain growth is provided by surface tension and is quanti-

tatively equal to  $\gamma/R$ , where  $R$  is the net radius of curvature of the grain boundary. The restraining force for each inclusion of radius  $r$  is  $2\pi r \gamma \sin \omega \cos \omega$  where  $\omega$  is the angle between the average surface of the grain boundary and the surface at the point where it joins the inclusion. For a maximum restraining effect,  $\omega$  is  $45^\circ$  and  $\sin \omega \cos \omega = \frac{1}{2}$ . The total restraining force acting on the boundary is the  $n_* \pi r \gamma$ , where  $n_*$  is the number of inclusions per unit area of grain boundary. Equating this to the driving force, we get as a condition for equilibrium that  $\pi n_* r R = 1$ . The surface density,  $n_*$ , is approximately  $n_* r$  where  $n_*$  is the number of particles per unit volume, or  $\frac{f}{(\frac{4}{3})\pi r^3}$  where  $f$  is the fraction of the total volume occupied by inclusions. Combining these relations we then have  $\frac{R}{r} \cong \frac{3}{4f}$ .

This, of course, is only an approximation, since inclusions are assumed to be spherical and of equal size and random distribution. It ignores the effect of inclusions located at grain edges and vertices, which must be more effective than at a surface. Nevertheless, to a first approximation, one can anticipate a definite relation between curvature of boundary (virtually equal to the grain size), the size of the inclusions, and the fraction of the total volume occupied by the inclusions. If a metal contains one percent by volume of inclusions, the grains cannot grow to a size more than approximately a hundred times that of the inclusions.

The only condition that would reduce the effect would be if the inclusions were angular in shape and had all their surfaces inclined at angles greater than  $45^\circ$  to all grain boundaries. If an inclusion can change its shape and establish a dihedral angle lower than  $180^\circ$  where it joins the boundary, its effect will obviously be greater than a spherical one of the same volume. Moreover, particles that appear as a result of transformation or precipitation

are likely to be concentrated at the grain boundaries. If inclusions are not absolutely rigid but can move somewhat, they will be collected on a grain boundary and move with it as it progresses. J. E. Burke has pointed out<sup>25</sup> that in the case of slightly soluble inclusions those located at a grain boundary will tend to grow at the expense of the ones in the body of the grain. For this reason, if a grain boundary temporarily stops moving because of a change of its edge geometry or otherwise, it will require more force to move it again than if it had continued in motion. Any factor tending to encourage collection of minor constituents of any kind at a grain boundary will decrease the grain size at which the boundary can no longer move.

On this picture, temperature does not change the relation between stable grain size and inclusion size although it does greatly affect the rate of approach to equilibrium. It will, however, have an effect on the rate of redistribution of inclusion material, and in many cases a higher temperature will result in complete solution of a material that had previously restricted growth.

As curvatures become less as growth occurs, there is also higher possibility that boundaries may be hung up on the slight energy hills caused by variation of surface energy with orientation of the boundary. All these factors can combine to produce the slowing and eventual cessation of normal growth when grains have reached a certain size, as observed by Beck,<sup>26</sup> Burke,<sup>25</sup> and others. Beck has also observed that grain growth stops when the grains have reached a size commensurate with the thickness of the piece being annealed. A decrease in growth rate would be expected on a two-dimensional basis because the curvatures are less and because there is a decreased number of edges on the average grain (6 instead of 36) which can lead to instability of the adjacent faces on their disappearance.

The behavior of grain boundaries at a

surface is striking evidence of the significance of surface energy and the general legitimacy of the analogy with soap films. A grain boundary always meets the surface of a piece of metal nearly perpendicularly (Fig 47) just as soap films meet a clean surface. Observed on the surface, the grains adopt a geometry not far from the ideal one in which boundaries join only at the true angle of  $120^\circ$ . This behavior can be seen in the distribution curves *A* and *C* of Fig 43. It is assumed that the slight deviations from ideal geometry result from variation of boundary energy with the orientations of the adjacent grains.

#### SOME PRACTICAL APPLICATIONS

Since the shape of microconstituents is a predominant factor in determining the physical properties of an alloy, it is obvious that there are almost no alloys in which surface tension is not of some importance.

The practical value of varying dihedral angles in connection with the control of the effect of impurities has already been indicated. The different behavior of various sulphides and oxides in steel can be explained directly in terms of surface energies and can be intelligently modified by proper understanding of the factors determining their distribution.

The principles discussed should be of practical value to the powder metallurgist. It is well known that the interstices of a porous solid compact will be filled with a liquid if the surface contact angle is less than  $90^\circ$ . The dihedral angle against a grain boundary is equally important. A mass of polycrystalline lumps will be disintegrated, not sintered together, by a liquid of zero dihedral angle, though capillary action will hold the mass as a whole together. A liquid of positive dihedral angle will act very differently from one with  $\theta = 0$ . In the case of a two-phase solid alloy made by powder metallurgy methods, the area of contact across which diffusion can occur will vary greatly with

the dihedral angle. The chance for grain growth will be greatly affected by impurities. The production of an alloy with connected channels, as in porous bearings, or with a continuous network of a given constituent, is possible only with the proper dihedral angle. It should be possible to produce porous bearings equivalent to the powder metallurgy product by displacing the liquid from a fine-grained alloy made by conventional casting methods, or by annealing a fine-grained worked alloy above its solidus.

The cracking of stressed metals in contact with molten solder or brazing solder is a direct result of low dihedral angle. Mercury will not crack steel as it does brass under stress, but brazing solder will crack either and molten lead neither. It should be possible to design a brazing alloy of high dihedral angle which would avoid completely the dangers of intercrystalline penetration and cracking, although such an alloy may have somewhat impaired wetting properties.

#### CONCLUSION

Despite the importance of surface tension effects in determining microstructure, it is not to be assumed that they are solely responsible for metal structures. Under many treatments time would be insufficient to achieve equilibrium of surface forces except in the immediate vicinity of the boundary. Concentration gradients will often intervene and inclusions will produce local distortion of the structures. The influence of residual strain in worked metals may also be significant. Though in alloys undergoing transformation, surface forces are of great significance, equilibrium dihedral angles are rarely obtained because coherency makes the surfaces strongly dependent on orientation. This effect, which has barely been discussed in the present paper, will certainly be found to be important in many cases, even including some two-phase alloys after working and

prolonged annealing. In fact, the structure of alpha-beta brass containing a small amount of beta (Fig. 11) shows many straight boundaries and an abnormally low dihedral angle, a fact that can only indicate some such orientation dependence. A far more elaborate analysis than has been given herein is necessary in elucidating such structures.

The above discussion has been based on relative values of interfacial tensions. No absolute values are known even for the energies of a metal crystal in equilibrium with its vapor, much less for grain and interphase boundaries, and no method at present available seems to be capable of determining this with any accuracy. Grain boundary surface energies are certainly small compared with those of free crystal surfaces. The ratio can be determined by measuring the dihedral angle of the groove formed where a grain boundary meets the surface.

No attempt has been made to cite all the literature dealing with surface tension of metals. Many writers have considered the role of surface tension as a driving force in grain growth, and a few have even contended that it is not important. The preferential adsorption of constituents at a surface—well known in aqueous systems—must result in the composition at the grain boundary being somewhat different from the body of the grain and must modify the surface tension composition relations. The significance of this has been discussed at length by Benedict<sup>27</sup> who believed that such adsorption is the primary reason for the effect of impurities on grain growth behavior.

#### ACKNOWLEDGMENTS

Practically every member of the staff of the Institute for the Study of Metals has contributed in some measure to the preparation of the present paper. Dr. Adam Skapski first incited the writer's interest in the significance of surface tension in solid

metals. The writer is particularly indebted to Professors Burke, Barrett, and Zener for opportunities to discuss the subject with them, with resultant clarification of many muddy statements. Most of the alloys for the study were made and heat treated by Messrs. K. K. Ikeuye and Werner Bergmann, whose assistance is gratefully acknowledged. The metallography was done by Mrs. Thelma Barkin Weinstock, who is adept at polishing and etching difficult two-phase structures in almost any system.

Part of the work described herein was done under Contract No. N-601-20-IV with the U. S. Office of Naval Research. The balance was made possible by University funds and the contributions of the industrial sponsors of the Institute for the Study of Metals.

#### REFERENCES

1. E. R. Parker and R. Smoluchowski: Capillarity of Metallic Surfaces. *Trans. A.S.M.* (1945) **35**, 362-371.
2. P. Schwarzkopf: *Powder Metallurgy* (1947) 167-168, New York.
3. D. Harker and E. Parker: Grain Shape and Grain Growth. *Trans. A.S.M.* (1945) **34**, 156-195.
4. C. Blazey: Brittleness in Arsenical Copper. *Jnl. Inst. Metals* (1929) **41**, 321.
5. E. Voce and A. P. C. Hallowes: The Mechanism of Embrittlement of De-oxidized Copper by Bismuth. *Jnl. Inst. Metals* (1947) **73**, 323-376.
6. F. Rhines: Discussion on Voce and Hallowes. *Jnl. Inst. Metals* (1947) **73**, 786-805.
7. T. H. Schofield and F. W. Cuckow: The Microstructure of Copper Containing Small Quantities of Bismuth. (1947) **73**, 377-384.
8. W. B. Price and R. W. Bailey: Bismuth—Its Effect on Alpha and Alpha-beta Brasses. *Trans. AIME* (1942) **147**, 136-143.
9. G. Quincke: Bildung von Zellen, Sphärokristallen und Krystallen. *Annal. Physik.* (1902) **9**, 1-43.
10. J. H. Watson: Liquidation or "Inverse Segregation" in the Silver-copper Alloys. *Jnl. Inst. Metals* (1932) **49**, 347-358.
11. J. W. Spretnak: Kinetics of Solidification of Killed Steel Ingots. *Trans. A.S.M.* (1947) **39**, 569-619.
12. C. Zener: Kinetics of the Decomposition of Austenite. *Trans. AIME* (1946) **167**, 550-583, *Metals Tech.* Jan. 1946.
13. M. L. V. Gayler and W. E. Carrington: Metallographic Study of the Precipitation of Copper from a Silver-rich Silver-copper Alloy. *Jnl. Inst. Metals* (1947) **73**, 625-640.

14. C. S. Smith: A.S.M. Symposium on Age Hardening. (1939) 425-426.
15. J. E. Burke and C. W. Mason: Recrystallization and Precipitation in Aging of Tin-bismuth Alloys. *Trans. AIME* (1942) 147, 300-309.
16. A. E. Flannigan, I. I. Cornet, R. Hultgren, J. T. Lapsley, and J. E. Dorn: Factors Involved in Heat Treating a Magnesium Alloy. AIME TP 2282. *Metals Tech.*, Sept. 1947. This volume, p. 524.
17. C. S. Smith and W. E. Lindlief: The Equilibrium Diagram of the Copper-rich Copper-silver Alloys. *Trans. AIME* (1932) 99, 101-114.
18. D. J. Mack: Isothermal Transformation of a Eutectoid Aluminum Bronze. TP 2242. *Metals Tech.* Sept. 1947. This volume, p. 240.
19. C. H. Desch: Second Report: The Solidification of Metals from the Liquid State. *Jnl. Inst. Metals* (1919) 22, 241-276. C. H. Desch: The Chemistry of Solid (Ithaca, New York, 1934). 53-68.
20. D'Arcy W. Thompson: On Growth and Form (Cambridge, 1942) Chapter VII.
21. F. G. Lewis: A Further Study of the Polyhedral Shapes of Cells. *Proc. Amer. Acad. Arts and Sciences* (1925) 61, 1-34.
22. E. B. Martzke: The Three-dimensional Shape of Bubbles in Foam-On Analysis of the Role of Surface Forces in Cell Shape Determination. *Amer. Jnl. Botany*. (1946) 33, 58-80.
23. William Thompson (Lord Kelvin): On the Division of Space with Minimum Partitional Area. *Phil. Mag.* (1887) 24, 503. (Collected Works, 5, 297.)
24. Clarence Zener (Inst. for the Study of Metals, Chicago): Private communication to the author.
25. J. E. Burke (Inst. for the Study of Metals, Chicago): Private communication to the author.
26. P. A. Beck, J. C. Kremer, L. J. Demer, and M. L. Holzworth: Grain Growth in High Purity Aluminum and in an Aluminum-magnesium Alloy. *Trans. AIME* TP 2280. *Metals Tech.* Sept. 1947. This volume, p. 372.
27. Carl Benedict: Die Kapillarität der Korngrenzen der Metalle, ihr Einfluss auf das Kornwachstum und ihre Bedeutung für den Stahl. *Koll. Ztsch.* (1940) 91, 217-232.